

Multi-constrained optimization combining ARMAX with differential search for damage assessment

Lakshmi K* and Rama Mohan Rao A^a

CSIR-Structural Engineering Research Centre, Chennai, Tamil Nadu, India

(Received November 9, 2018, Revised May 31, 2019, Accepted August 3, 2019)

Abstract. Time-series models like AR-ARX and ARMAX, provide a robust way to capture the dynamic properties of structures, and their residuals can be effectively used as features for damage detection. Even though several research papers discuss the implementation of AR-ARX and ARMAX models for damage diagnosis, they are basically been exploited so far for detecting the time instant of damage and also the spatial location of the damage. However, the inverse problem associated with damage quantification i.e. extent of damage using time series models is not been reported in the literature. In this paper, an approach to detect the extent of damage by combining the ARMAX model by formulating the inverse problem as a multi-constrained optimization problem and solving using a newly developed hybrid adaptive differential search with dynamic interaction is presented. The proposed variant of the differential search technique employs small multiple populations which perform the search independently and exchange the information with the dynamic neighborhood. The adaptive features and local search ability features are built into the algorithm in order to improve the convergence characteristics and also the overall performance of the technique. The multi-constrained optimization formulations of the inverse problem, associated with damage quantification using time series models, attempted here for the first time, can considerably improve the robustness of the search process. Numerical simulation studies have been carried out by considering three numerical examples to demonstrate the effectiveness of the proposed technique in robustly identifying the extent of the damage. Issues related to modeling errors and also measurement noise are also addressed in this paper.

Keywords: Damage assessment, multi-constraint optimization, time series analysis, ARMAX model, cepstral distance, Subspace angles, measurement noise

1. Introduction

Damage detection is based on the premise that damage in the structure will cause changes in the dynamic characteristics of the structure and reflect in the measured vibration data. The step by step process of SHM involves the determination of the comprehensive health of the structure by identifying the presence, location, extent of damage and the assessment of the useful remaining life of the structure. Doebling *et al.* (1998), Sohn *et al.* (2003) and structural health monitoring conferences (Akhras *et al.* 2008) have provided an extensive literature of various methods and advancements of SHM. Majority of the methods, based on the vibration measurements (Li and Chen 2013) make use of modal parameters (Homaei *et al.* 2014) like natural frequency, mode shapes, the curvature of mode shapes, modal strain energy, flexibility (Nobahari and Seyedpoor 2013) and FRFs (Huynh *et al.* 2005). Multivariate techniques such as principal component analysis (Rao *et al.* 2012), soft computing techniques like Artificial neural networks (ANN) (Hore *et al.* 2016), evolutionary techniques like genetic algorithms (Koh and Perry 2009, Laier and Morales 2009) and differential

evolution (Seyedpoor and Montazer 2016) are also being used in damage detection recently. Methods based on time scale analysis like wavelets (Bagheri *et al.* 2011, Hamidian *et al.* 2018) or time-frequency analysis such as Hilbert-Huang transform (HHT) (Bao *et al.* 2009) are also being popularly employed.

A major challenge in structural health monitoring (SHM) is distinguishing the effects of damage on structural behaviour from the effects of environmental and operational variation (EOV). Real-world structures are exposed to constantly changing conditions, and therefore, methods robust to the effects of EOV must be established, for SHM to be practical. Environmental and operational variability is usually handled by framing the SHM problem as a novelty detection problem, in which a model for healthy structural behaviour is established and new observations are classified as healthy or damaged depending on whether or not they continue to follow that model. An alternative approach is to preprocess the measured raw data to identify combinations of features invariant under environmental variability. Techniques like PCA, nonlinear PCA and cointegration can be applied for this purpose. The third alternative is to learn commonalities across different conditions to explicitly model the individual behaviours of the structure under different environmental variability.

Recent trends in SHM are towards the application of statistical signal processing techniques to diagnose damage (Sohn and Farrar 2001, Carden and Brownjohn 2008). Such methods rely on the signatures obtained from the recorded

*Corresponding author, Ph.D.

E-mail: lakshmik@serc.res.in

^a Ph.D.

vibration, strain or other data to extract features that change with the onset of damage. These features can then be discriminated in a pattern classification framework. Time-series models provide a robust way to capture the dynamic properties of structures, and their residuals can be effectively utilized as features for damage detection. The AR-ARX or ARMA models are useful not only in the univariate case but can also be applied to damage detection in multivariate time series, such as those generated by sensor networks. Further, it is rather more comfortable to handle environmental variability in these time series models, as the method of constructing “lookup table” of measured data can be used to enumerate normal behaviour under a range of environmental and operational conditions. The model residuals of the reference model that most closely resembles the new observations are then used to evaluate the health of the structure. A considerable amount of research (Yu and Zhu 2015, Lakshmi and Rao 2014, Zheng and Mita 2008, Lakshmi and Rao 2015, Lakshmi and Rao 2016, Cheng *et al.* 2017, Tang *et al.* 2018) is reported in developing various damage diagnostic techniques using time series models. Majority of them use AR-ARX models or ARMA models for damage diagnostics. Most of these time series models are used for detecting the time instant of damage and also possibly the spatial location of the damage. However, these techniques have not been further exploited to estimate the extent of the damage.

In this paper, a technique to estimate the extent of damage by combining time series models with a new variant of differential search optimization technique is presented. In the literature, inverse problems related to the quantification of damage are often solved using unconstrained optimization problems during structural parameter estimation or damage assessment. Now, it is formulated as a multi-constrained optimization problem in order to improve the robustness of the identification process with modeling errors and also with the measured acceleration time history signals contaminated with noise. In this paper, the vibration responses are modeled with ARMAX time series model. However, the same technique can be used even with other time series models like AR-ARX and ARMA.

In this paper, first, the basic mathematical structure of the ARMAX model is presented, followed by the damage detection process. As the details related to ARMAX models are already reported in the literature, they are discussed very briefly for the sake of completion. This is followed by the formulation of the objective function and constraints for optimization. The basic differential search algorithm and a new variant of differential search algorithm with substantial enhancements proposed in this paper are presented in the next section. Numerical simulation studies have been carried out by solving three numerical examples to demonstrate the effectiveness of the proposed technique while dealing with noise contaminated signals and also with modeling errors.

2. ARMAX model and damage index

The ARMAX model is preferred in this paper because it

includes the dynamics of the disturbance also, unlike the other time series models. An ARMAX process of a healthy acceleration time history data, $x(t)$ is given below.

$$x(t) = \sum_{i=1}^p \alpha_i x(t-i) + \sum_{i=1}^q \beta_i u(t-n_k-i) + \sum_{i=1}^b \delta_i \varepsilon(t-i) + \varepsilon(t) \quad (1)$$

where ε is the prediction error between the measured signal and the signal from the prediction model, n_k is the time delay, equal to 1. α_i , β_i and δ_i , are the parameters of AR, exogenous input(u) and MA models with p , q and b as their orders respectively. While fitting an ARMAX model, to the acceleration time history data from a sensor node, the input series, u , is the acceleration time history signals of adjacent sensor nodes.

A damage index, which is based on the distances of ARMAX models of the pristine and current data is evaluated, to detect the presence and spatial location of the damage. The distance measure between the two-time series models is considered to be correlated with the position and severity of the damage. To measure the distance, the cepstral distance, which is the weighted Euclidean distance between the power cepstrum of ARMAX models of the two subsets is used.

Balsamo *et al.* 2014, highlight the features of cepstral coefficients for feature extraction. The procedures followed in extracting the cepstral features are grossly contrast to the methods generally used in SHM. The extraction of cepstral features is through digital signal processing techniques and do not require system identification techniques or defined optimal modal parameters, which are generally arrived using computationally intensive procedures. As cepstral coefficients are evaluated from the logarithm of the spectrum of response time histories from a structure, they are strongly related to the features of the properties of the structure. Unlike AR coefficients, the number of cepstral coefficients considered does not alter the results of damage diagnosis and therefore seen as a more reliable feature.

The mathematical formulations of the cepstral distance based damage index are already reported in the literature and are presented briefly in Appendix - A, for the sake of completeness. This cepstral distance measure evaluated from Eqn. (A5) is used for damage localization and is calculated for all the sensor nodes independently. Once the damage index (cepstral distance) of the subset for all the sensor nodes are obtained, the spatial location of damage can be identified. The cepstral distance increases with the increase in the difference between any two signals considered for investigation. Therefore, the value of the higher damage index at a sensor node is considered to be an indication of the presence of damage near that node on the structure. The time instant of damage can be calculated from the subset index number of the current dataset. Therefore, the damage index based on the cepstral distance between the current and reference (baseline) data can act as a good localization metric as it clearly reflects the change in the dynamic state of the structure near each measured sensor node without any spatial correlation.

3. Quantification of damage

Once the spatial damage is identified using the cepstral distance between the ARMAX models constructed using the current and the pristine measured acceleration time history data, the multi-constrained optimization problem, to quantify the damage extent, is performed. As mentioned earlier, damage detection is based on the premise that damage in the structure will cause changes in stiffness. Accordingly, the stiffness reduction factors (β) are considered as design variables.

The structural damage is modeled at the parametric element-level, by expressing the stiffness matrix of the damaged j th element as

$$K_j^d = \beta_j K_j^u \quad (2)$$

where $\beta_j \in [0,1]$ refers to the reduction in the stiffness matrix of the j th element, K_j^u , refers to the stiffness matrix of the j th element before the damage. The global stiffness matrix can be written as

$$K = \underset{j=1}{\overset{n_{el}}{A}} K_j \quad (3)$$

where A is the assembly operator used in assembling the contribution of the total elements, n_{el} , in the finite element method. The cost function based on the AR parameters of ARMAX time series models is given by:

$$F1 = \left(\sum_{j=1}^p abs \left(\frac{AR_d(j)}{\max(AR_d)} - \frac{AR_s(j)}{\max(AR_s)} \right) \right) \quad (4)$$

Where AR_d and AR_s are the AR parameters of ARMAX models fitted to the measured acceleration data and simulated acceleration data with a trial set of reduction factors of the elements respectively and p is the AR order determined by partial autocorrelation functions.

The cost function specified in the Eqn. (4) may not be sufficient for a better convergence and to obtain the optimal solution in the presence of environmental variability and measurement noise another cost function which is based on principal component analysis using Singular value decomposition (Lakshmi and Rao 2014) of the dataset is proposed as below.

$$F2 = \left[\sum_{j=1}^n abs \left(\frac{PC_d(j)}{\max(PC_d)} - \frac{PC_s(j)}{\max(PC_s)} \right) + \sum_{j=1}^n abs \left(\frac{SV_d(j)}{\max(SV_d)} - \frac{SV_s(j)}{\max(SV_s)} \right) \right] \quad (5)$$

where PC_d is the principal component of measured acceleration data, PC_s is the principal component of simulated acceleration data, SV_d is the singular values of principal component for measured data, SV_s is the singular values of principal component for simulated data, and 'n' is the number of principal components.

The final cost function (i.e., objective function) used in the present work is based on the time series parameters and

the principal components, given as:

$$Cost\ Function = \min [F1 + F2] \quad (6)$$

Since it is proposed to formulate the optimization problem as a multi-constrained optimization problem, both cepstral distance between ARMAX models and the principal angle between the subspaces are used as constraints. The details related to principal angle between the subspace spanned by the measured responses and analytical responses with the stiffness coefficients of a typical solution provided by meta-heuristic algorithm during optimization are given in Appendix-A. A newly proposed variant of the differential search algorithm for solving the proposed multi-constrained optimization problem is used.

4. Differential Search Algorithm (DSA)

Once the spatial location of the damage is identified using the cepstral distance of ARMAX models, the extent of damage (i.e. quantification of damage) at the identified locations is assessed, by using inverse computational algorithms. However, recently, this class of inverse problems is being popularly solved using meta-heuristic algorithms by formulating the associated inverse problem as an optimization problem. In the present work, a similar procedure is followed. The present inverse optimization problem requires the measured time history responses from the structure of interest in order to arrive at the severity of the damage. Field measurements obtained will obviously be corrupted by noise. Hence, the optimization algorithm employed should exhibit less sensitivity to measurement noise. Further, the optimization problem associated with damage quantification is extremely complex, multi-modal and nonlinear, hence there is a need to carefully select the suitable meta-heuristic algorithm for this kind of problems. Further, to incorporate in the SHM scheme, apart from finding the globally optimal solution, the algorithm should also have the capability of faster convergence.

Several meta-heuristic algorithms are reported in the literature and the majority of them are applied to solve inverse problems. However, the majority of meta-heuristic algorithms have several parameters to adjust so that the convergence characteristics can be improved by balancing the diversification and intensification process. In this paper, a vastly improved version of differential search algorithm originally proposed by Civivioglu (2012) is used. Differential search is a much recent one among the algorithms proposed, based on swarm intelligence and reported to be effective in dealing with multimodal optimization problems. Apart from this, unlike many meta-heuristic algorithms, the differential search has few parameters to adjust for optimal performance. Further, it is reported that the differential search converges faster than several other recent swarm intelligence algorithms (Liu *et al.* 2015). However, there are still some shortcomings in the classical differential search algorithm. This algorithm is built with extremely good diversification mechanism. However, intensification mechanism is rather weak. This lack of effective exploitative mechanism may lead to slow convergence in some complex optimization problems at later

stages. It is proposed to improve the intensification mechanism in the basic differential search algorithm by augmenting with a neighborhood search algorithm. It is known very well that in general, meta-heuristic algorithms cannot outperform the specialized neighborhood search algorithms. Nevertheless, the neighborhood search methods face initialization problem most of the cases. Precisely, the local optimizer performs based on the function of the initial solution. Therefore, combining a meta-heuristic algorithm with an efficient neighborhood search algorithm is expected to provide a much better solution for the reason that the good initial solutions for the neighborhood search algorithm are provided by the meta-heuristic algorithms for further exploration.

Hence in this paper, a vastly improved meta-heuristic algorithm by augmenting with adaptive features, augmenting with a powerful neighborhood search algorithm and also with a dynamic exchange of information is presented. The proposed features enhance the intensification mechanism of the algorithm and thereby strike a good balance between intensification and diversification. This will result in faster convergence and also provide a globally optimal solution. First, the basic DSA algorithm will be presented followed by the improvements made in the proposed algorithm.

4.1 Basic DSA

Similar to any other optimization algorithm based on stochastic search, DS algorithm, made up of random solutions of the respective problem, corresponds to an artificial superorganism migrating to the global optimum solution of the problem. This algorithm is developed by drawing inspiration from the seasonal migration of living organisms in search of ideal sources for food. Since the quality and quantity of food will obviously vary from season to season, due to the periodical climatic changes, this migration takes place throughout the year and move from poor region to suitable and efficient habitat where capacity and diversity of natural sources are high. A large number of migrating living organisms constitute the superorganism. The differential search algorithm simulates the Brownian-like random-walk movement to describe the search mechanism during migration.

The artificial superorganism (consists of a population of generated random solutions), during the migration process, explores the randomly selected positions (places) for their suitability for temporary settlement. If a suitable temporary stopover position is found during the migration by the members of the artificial-superorganism (i.e. artificial-organisms) immediately migrates to the new position and continue their migration process from this newly discovered position. The migration process of the superorganism will continue from the current position. The basic steps involved in differential search algorithms are:

In DSA, each of the artificial organisms represents a possible solution $V_i = (v_{i1}, v_{i2}, v_{i3}, \dots, v_{iD})$ ($i=1, N$) where N signifies the number of artificial organisms in the superorganism and D depends on the number of design variables to define the specific optimization problem on hand. Initially, all the solutions (artificial organisms) are generated randomly. Accordingly, the initial position of each artificial organism can be defined by using upper and lower limits of each design variable of the optimization problem on hand

$$v_{ij} = \text{Lower}_j + \text{rand} * (\text{Upper}_j - \text{Lower}_j) \quad (7)$$

where Upper_j and Lower_j are the user-defined upper and lower bounds of the j th design variable.

The search mechanism for finding the stopover sites at the areas in between the artificial-organisms follows the Brownian-like random walk model. In order to discover the new stopover site, the individuals are chosen to randomly (artificial organisms) move towards the targets of the donor. The order of the number of the elements in the set is randomly changed each time through random shuffling. The positional change (i.e., stopover position) of the artificial organisms is controlled by a value 'scale'. Accordingly, the stopover vectors (St) for each artificial organism are computed as

$$\text{St}_{ik} = V_{ik} + \text{scale} * (V_{dk} - V_{ik}) \quad (8)$$

where d is the donor, $d \in [1, 2, \dots, N]$ are randomly chosen integers obtained using the *random_shuffling* function and $d \neq i$. It must be mentioned here that the value of scale is produced by a gamma random number generator (i.e., randg) controlled by a uniform distribution random number generator (i.e., rand) in the range of 0 and 1.

The stopover site is controlled to remain in the determined search space range. In DS algorithm, the stopover site found by the search process is evaluated and if the newly discovered stopover site of an artificial organism has better quality than the current sources of that artificial-organism, it goes to that stopover site. The stopover position (site) can be calculated by the artificial organisms of the superorganism and can be determined as

$$\tilde{\text{St}}_{ij}^g = \begin{cases} \text{St}_{ij}^g & \text{if } R(i,j)=0; \\ v_{ij}^g & \text{if } R(i,j)=1; \end{cases} \quad (9)$$

where $j=[1, 2, \dots, D]$; $R(i, j)$ is an integer number either 0 or 1. $\tilde{\text{St}}_{ij}^g$ is the trial vector of the i th particle in the j th dimension at the g th generation. While the artificial organisms of a superorganism change site, that respective superorganism continues its movement towards the global optimum. The new population (i.e., $g=g+1$) is chosen between the stopover site population and the artificial-organism population using the following selection process.

$$V_i^{g+1} = \begin{cases} \tilde{\text{St}}_i^g, & \text{if } f(\tilde{\text{St}}_i^g) \leq f(V_i^g); \\ V_i^g, & \text{if } f(\tilde{\text{St}}_i^g) > f(V_i^g); \end{cases} \quad (10)$$

It should be mentioned here that the differential search algorithm may simultaneously use more than one individual unlike other stochastic algorithms like differential evolution (DE) or Artificial Bee Colony (ABC) algorithm. Similarly, DSA has no inclination to correctly move towards the best possible solution to the problem which is in contrast to the behavior of DE, ABC or particle swarm optimization (PSO) algorithm. In view of this, DSA is more adaptive towards finding multi-modal solutions

4.2 Adaptive DSA

The differential search algorithm is reported to have a better capability in terms of exploring search spaces when compared to other population-based meta-heuristic algorithms especially while dealing with multi-modal optimization problems. However, there are still some limitations in the classical DS algorithm. Even though the DSA is built with better exploration capabilities, it is rather weak in the exploitation of the solution. In view of this, the convergence rate is rather slow in some instances. Major attributes of any successful meta-heuristic algorithms are strong exploitation and exploration capabilities and striking a good balance between them in order to accelerate the convergence rate and at the same time preventing the algorithm from premature convergence. Hence the majority of the efforts in algorithmic research are devoted to enhancing the exploitation capability while simultaneously building up good exploration capability in order to accelerate convergence rate and avoid premature convergence. In the initial stages, of execution, the algorithm should exhibit high diversification capability in order to explore the search space vigorously and at the later stages i.e. near convergence, the intensification capability should be high with low or marginal diversification for faster convergence to the optimal solution.

The control parameters play an important role in all the meta-heuristic algorithms to improve the convergence rate and also preventing premature convergence. One of the major advantages of DSA is that there are only two control parameters i.e., p_1 and p_2 in the DSA algorithm, unlike many popular meta-heuristic algorithms. Earlier investigations on these control parameters indicate that they depend on the complexity and also the particularity of the problem on hand. In the majority of the cases, these two parameters P_1 and P_2 are set to $(0.3 \cdot \text{rand})$ to obtain good results. However, in the present work, it is proposed to adjust the values of these two control parameters dynamically during the search process based on the feedback on the improvements in the fitness values (rather convergence rate). These adaptive features built into the proposed algorithm certainly enhances the convergence rate of the solution, by ensuring a good balance between exploitation and exploration.

4.3 Hybrid adaptive differential Search algorithm (HADS algorithm)

The exploitation capability of the classical differential search algorithm is rather weak and it requires strengthening. Keeping this in view, it is proposed to augment the adaptive differential search algorithm with a local search algorithm in order to substantially enhance the exploitation capabilities. It should be mentioned here that the meta-heuristic algorithms including the present differential search cannot compete with a promising local search algorithm (Rao and Lakshmi 2011) in obtaining an optimal solution without converging to local optima. However, the major limitation of the local search algorithms lies in the selection of the good initial point in the search space i.e., initialization problem. Hence the performance

of these local search algorithm is always a function of the initial solution to which it is applied. The exemplary capabilities of these local search algorithms can be exploited, by feeding good potential initial points identified using meta-heuristic algorithms to exploit the search space and provide improved solutions. The resulting hybrid algorithms (i.e., a meta-heuristic algorithm combining with local search algorithm) will obviously exhibit superior convergence capabilities. Keeping this in view the proposed adaptive DSA is combined with a popular non-gradient based local search algorithm called Nelder-Mead (NM) algorithm shown in Figure 1. Alternatively, Hooke and Jeeves algorithm (Hooke and Jeeves 1961) in the place of the Nelder-Mead algorithm is used, to investigate the comparative performances of these popular local search algorithms. The flowchart of Hooke and Jeeves algorithm is given in Figure 2. The flowchart of the resulting hybrid adaptive differential search algorithm given in Figure 3 details the computational procedure associated with it.

Hybridizing with a local search algorithm will enhance drastically the exploration capabilities (Johnson and McGeoch 1997). However, it may take away the balance between exploitation and exploration and thereby effects the performance of the algorithm and its efficiencies. More focus on the exploitation due to the augmentation of local search requires the exploration to be limited to only a part of the search space. This may result in an increased probability of getting trapped in local optima. Keeping this in view, the convergence characteristics of the HADS algorithm are further improved by formulating a new version of the differential search algorithm with dynamically changing subpopulations. The details of the proposed hybrid adaptive differential search algorithm with dynamically changing subpopulations are presented in the next sub-section.

4.4 Hybrid adaptive differential search with multi superorganisms

The classical differential search algorithm basically works with single superorganism. There is sufficient evidence in the literature to indicate that meta-heuristic algorithms with models comprising of multiple small populations perform better than a single population model (Johnson and McGeoch 1997). Island models developed for evolutionary computing techniques is also another example of successful implementation of multi-population models which are generally found superior to their single population counterparts (Rao and Lakshmi 2012). Inspired by these facts, a new differential search algorithm with multiple superorganisms, each with a small number of organisms is proposed, in order to maintain faster convergence while maintaining larger diversity during the search. Since the organisms in each sub-superorganism dynamically migrate to other sub-superorganism, the proposed algorithm is termed as a differential search algorithm with dynamic superorganisms. In the proposed algorithm, the randomly generated artificial organisms at the initial stage are grouped into small sized sub-superorganism, with each consisting of an equal smaller number of artificial organisms. Each sub-superorganism

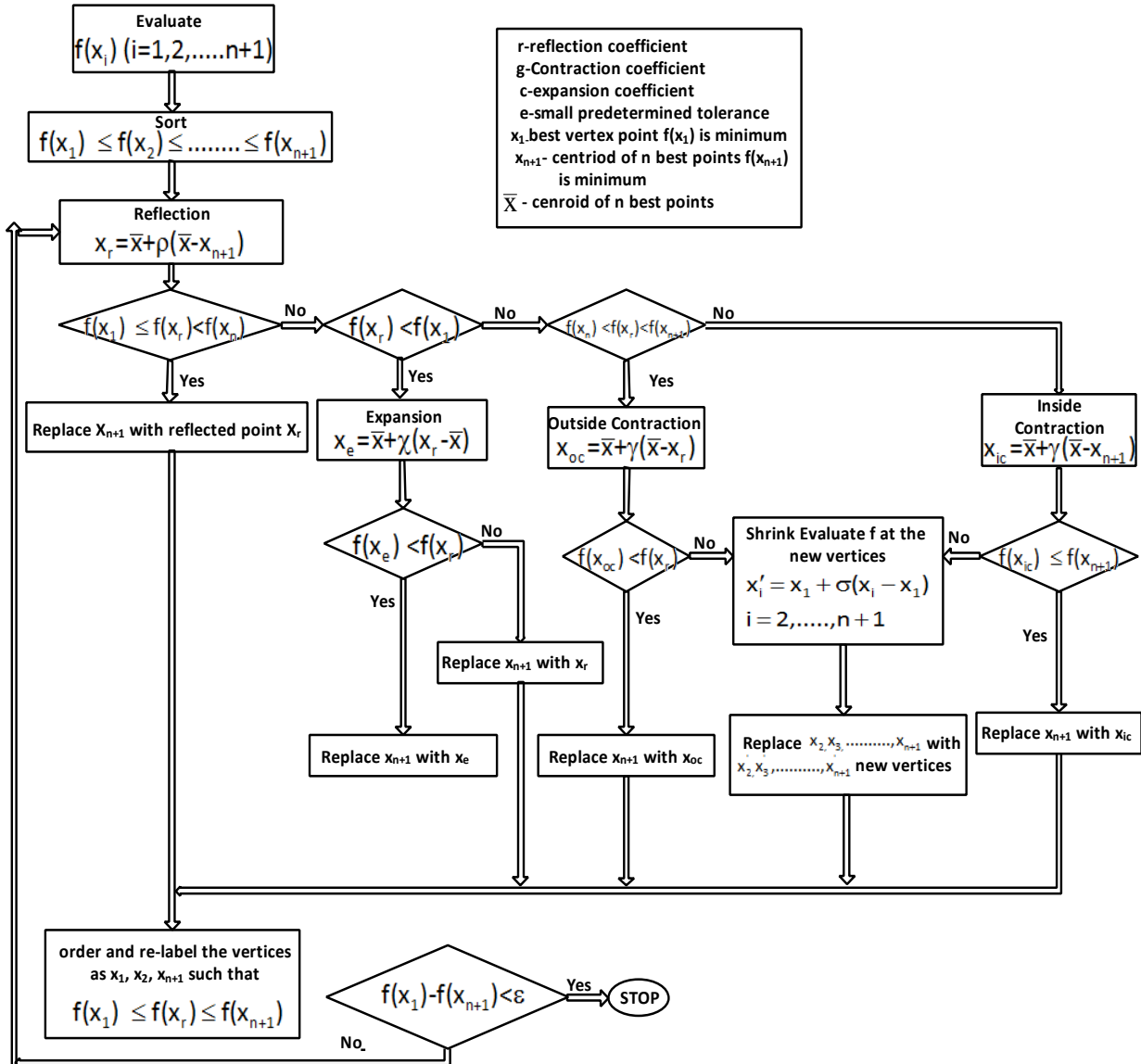


Fig. 1 Nelder-Mead algorithm

uses its own artificial organisms to migrate to new stopover sites using the search process associated with the hybrid adaptive differential search explained in the earlier section using their own best historical information. Since the number of artificial organisms is small in number, the solution is likely to converge to a local optimum. In order to avoid this premature convergence, the information needs to be exchanged across sub-superorganisms. It is also mandatory to maintain higher diversity in the sub-superorganisms while exchanging information. To ensure this, a neighborhood structure for the artificial organisms in each sub-superorganism, which changes dynamically, is proposed through a shuffling schedule. Accordingly, the population is shuffled after 'm' generations, defined by the user, and the process of migration to the next stopover site is continued in the pursuit of reaching the optimal solution.

Exchange of information of each sub-superorganism during the previous regrouping period 'm' takes place after every 'm' trials. The search process in each artificial

superorganism is carried out using the proposed hybrid adaptive differential search algorithm shown in Figure 3. However, different control parameters are used at the start in each sub-superorganism which may change adaptively during the search process. The parallel search involved in the proposed multi sub-superorganism model with a dynamic exchange of information across sub superorganisms accelerates the search process towards an optimal solution. It should be mentioned here that the exploration capabilities are significantly enhanced in the proposed algorithm through parallel search and dynamic exchange of information among the sub superorganisms. The exploitation capabilities are also significantly enhanced by augmenting with an effective local search algorithm like the Nelder-Mead algorithm. The complete details related to the computational procedure associated with the proposed hybrid adaptive differential search with multiple sub superorganisms is presented in the flowchart shown in Figure 4.

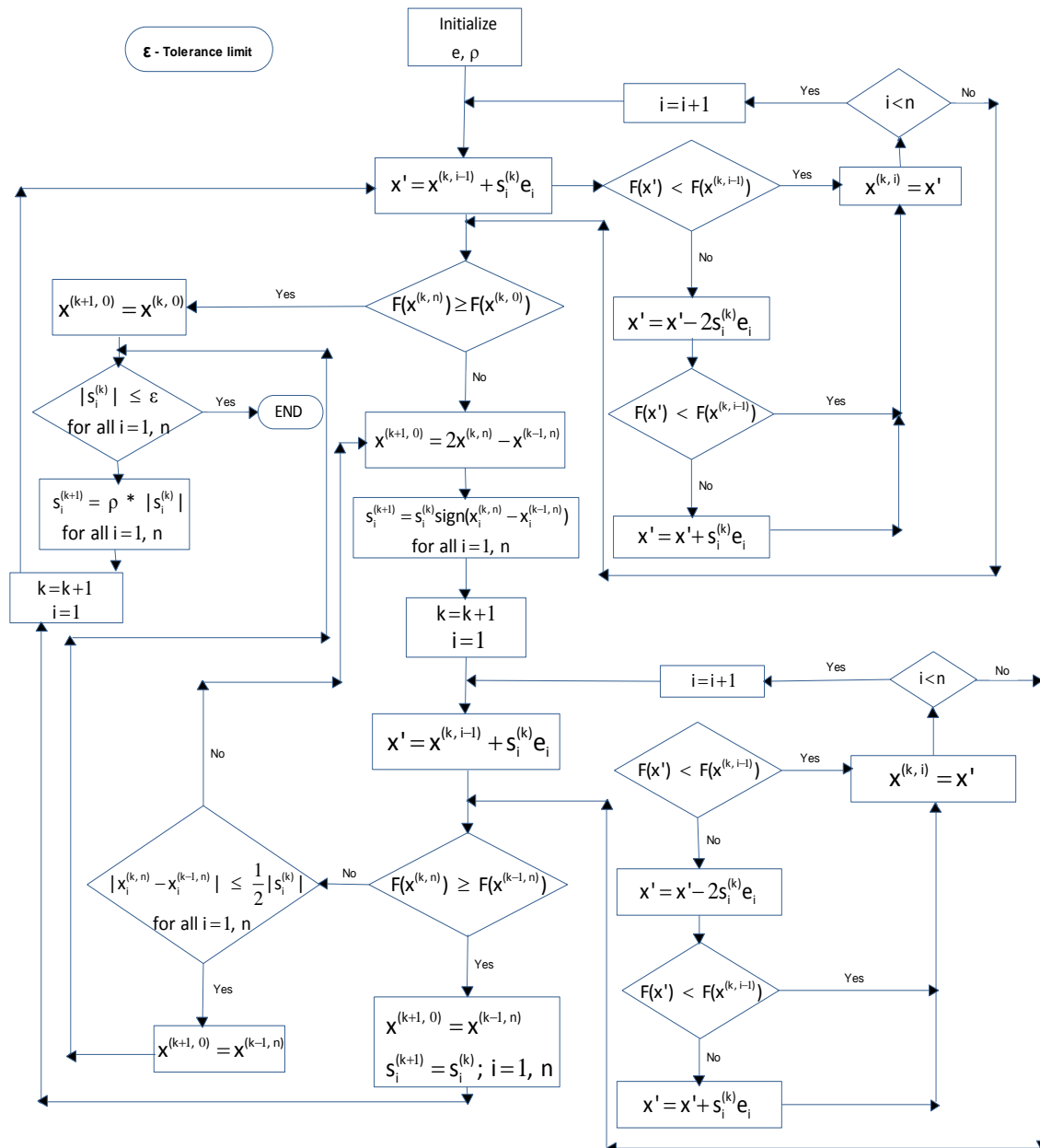


Fig. 2 Hooke and Jeeves Algorithm

In order to accelerate the convergence rate further and also to improve the accuracy of the parameter identification process, it is attempted to shrink the search space during the course of execution of the proposed algorithm. Shrinking the search space has been successfully used in several earlier investigations (Chakraborty and Dutta 2005, Rao and Lakshmi 2012). In the present work also, it is proposed to shrink the search space based on the history of best solutions obtained in the earlier evolutions. The procedure outlined earlier in Jayalakshmi *et al.* (2018) is adopted.

5. Complete damage diagnostic procedure

The proposed damage diagnosis involves the processes of (i) Damage detection (ii) Damage quantification at

identified locations using DHADS optimization algorithm. The step by step process is as given below:

In the damage detection phase, the time instant and the spatial location of damage are identified using time series analysis of ARMAX models.

i. Formation of pristine data: The baseline data ($X(t)$) is basically the acceleration time history data generated when the structure is in its healthy state under varying environmental and operational conditions and also measured at different times. This pristine data is partitioned into a convenient number of smaller subsets and it forms a huge collection of samples

ii. Construction of the ARMAX model with pristine data: For each subset, the data is fitted to the ARMAX model using Eqn. (1).

iii. Formation of current data: The current data

subsets ($Y(t)$) is created from the acceleration data from the unknown state of the structure (i.e., healthy or damaged state).

iv. Fitting ARMAX model to current data: Employing the new current time series, ($y(t)$), collected from the system of the unknown structural condition, the ARMAX model is constructed as

$$y(t) = \sum_{i=1}^p \alpha_i y(t-i) + \sum_{i=1}^q \beta_i u(t-nk-i) + \sum_{i=1}^b \delta_i \varepsilon(t-i) + \varepsilon(t) \quad (11)$$

v. Normalisation: This is carried out to ensure that every subset of the current data is paired with a subset of a baseline (pristine) data, such that they possess closely similar conditions of unmeasured variability, if not the same. Here, the AR coefficients of the ARMAX models are used for this purpose. Every subset of the current data, $y(t)$ is matched with any one of the subsets of the baseline data, $x(t)$ using the 'p' lagged AR coefficients, ϕ , of their ARMAX models, on the basis of their correlation values.

$$Difference = \sum_{j=1}^p (\phi_x^j - \phi_y^j)^2 \quad (12)$$

vi. Evaluation of Damage Index: The damage index using Cepstral distance (Eqn. A5) between the ARMAX models of current and the matched pristine data is evaluated for each sensor node. The magnitude of the cepstral distance increases with the presence of damage and therefore, the sensor node which is located near the damage, shows the largest magnitude of the cepstral distance measure when compared to other sensors. Thus the location of the damage is identified precisely.

vii. Detection of the extent of the damage: Based on the identified location of damage in step (vi), the extent of damage is estimated, by solving the multi-constrained optimization problem using the newly developed Dynamic Hybrid Adaptive differential Search (DHADS) algorithm. The cost function is given in Eqn. 6 with constraints as the cepstral distance of ARMAX models and the subspace angle spanned by the measured and the simulated responses. The stiffness reduction factors corresponding to elements, identified with damage are considered as design variables. Alternatively, stiffness reduction factors corresponding to all the elements can be used as design variables in order to robustly identify the spatial location and damage extent using the proposed constraint optimization formulation. The upper and lower limits of design variables are considered as 0.1 and 2.0 respectively.

The complete process of damage diagnosis including the design variables, cost function, and the constraints are shown in Figure 5.

5.1 Damage diagnosis with limited instrumentation

Data-driven algorithms like time series models can be effectively exploited using dense sensor networks which provide high-resolution information of the structure.

However, due to cost and accessibility issues, the number of sensors placed on the structures will be restricted. The minimum number of sensors that are to be placed on the structure should always be higher than the number of modes being excited. Once the number of sensors is selected, it is necessary to identify the optimal locations on the structure, in order to capture the complete dynamics of the system with least redundancy from the measured time history responses. In view of this, for a successful Structural Health Monitoring System, the placement of the sensors at critical spatial locations on the targeted structure is the crucial issue.

The optimal sensor placement methods are based on the mode shapes of the pretext finite element model (FEM). The aim of these methods is to optimize the sensor locations to extract the desired number of modes and other important parameters like structural damping, dynamic forces acting on the structure are not accounted for. In this paper, the efforts are directed towards obtaining the optimal sensor locations considering the input excitation force as well as damping apart from the other dynamic characteristics of the structure. The principal component analysis is employed for this purpose and the formulations closely follow the Effective Independence approach (Kammer, 2005, ARM Rao and Ananda Kumar, 2008). The basic difference lies in using principal components instead of mode shapes to account for input excitation location and damping.

Principal Component Analysis (PCA) is a multivariable analysis technique, which provides arguments to reduce the original complex data set to a lower dimension. Also, some of the hidden and simplified structure/patterns that often underlie it are revealed by PCA. PCA aims to find out the important dynamic characteristics and redundant noise components in the system (Worden and Farrar, 2007). From the dynamic time history response, principal components can be computed by performing the singular value decomposition (SVD) on the measured dynamic time history response from the sensors placed spatially across the structure. Using the SVD, the dynamic time history response data A (Nxn matrix of data, with n data points at N different spatial locations on the structure), can be decomposed as

$$A = U \Sigma V^T \quad (13)$$

where the matrix U of size NXN are the principal components(PCs), V of size nxn is the principal coordinate matrix and Σ of size, N X n is a diagonal matrix, in which the singular values are arranged in the decreasing order of their magnitude. Each of the singular value present in the diagonal of the matrix Σ represents the energy present in the corresponding mode. The first few singular values based on energy criteria corresponding to 99% of total energy (Feeny and Liang 2003) are generally used to characterize the structural system.

In contrast to effective independence method (Efi), where mode shapes are used to obtain the optimal sensor locations, in the present work, principal components are used for the following reasons. Optimal sensor placement technique (i.e., Efi) based on mode shapes, represent the

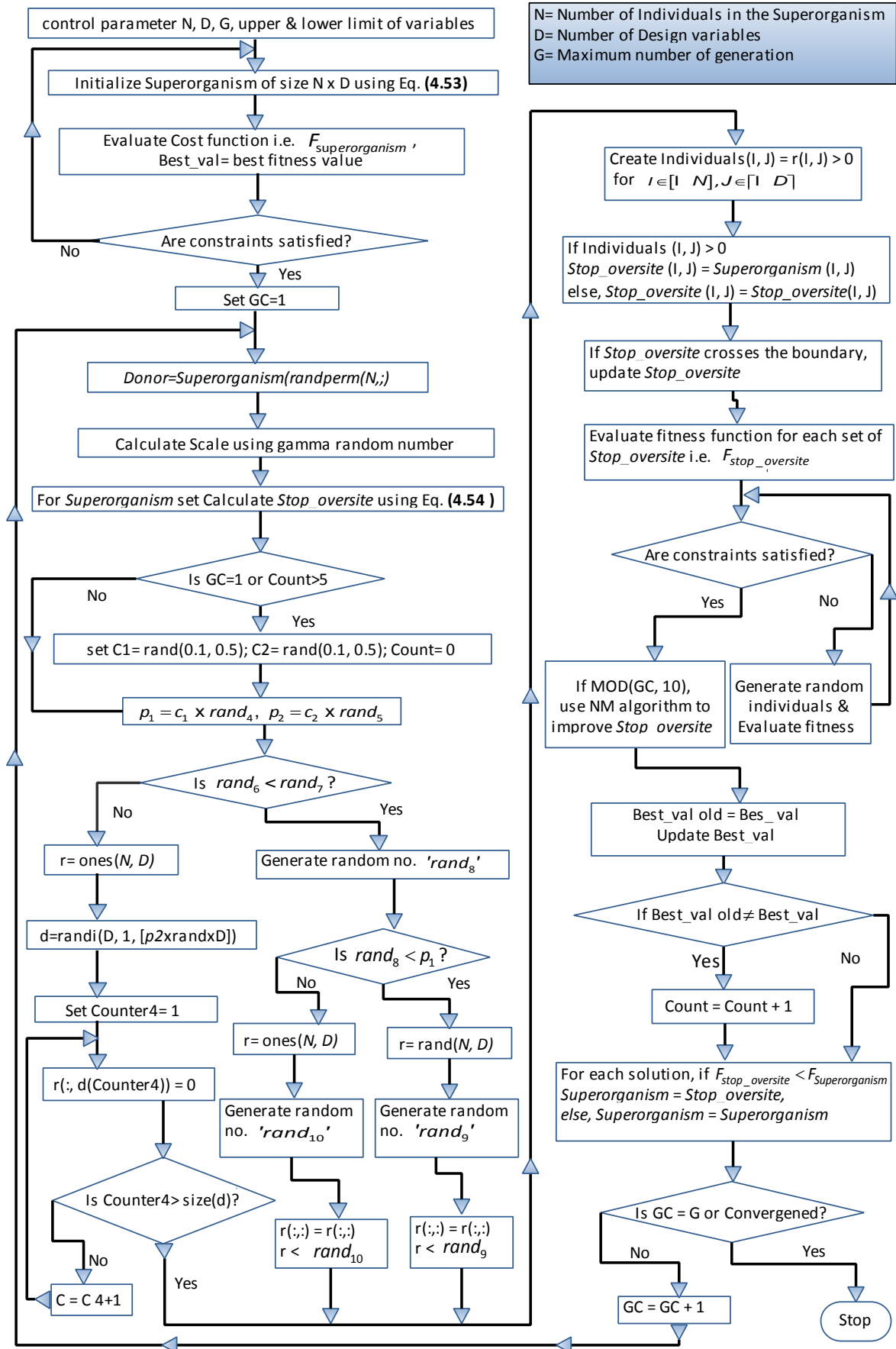


Fig. 3 Hybrid adaptive Differential search (HADS) algorithm

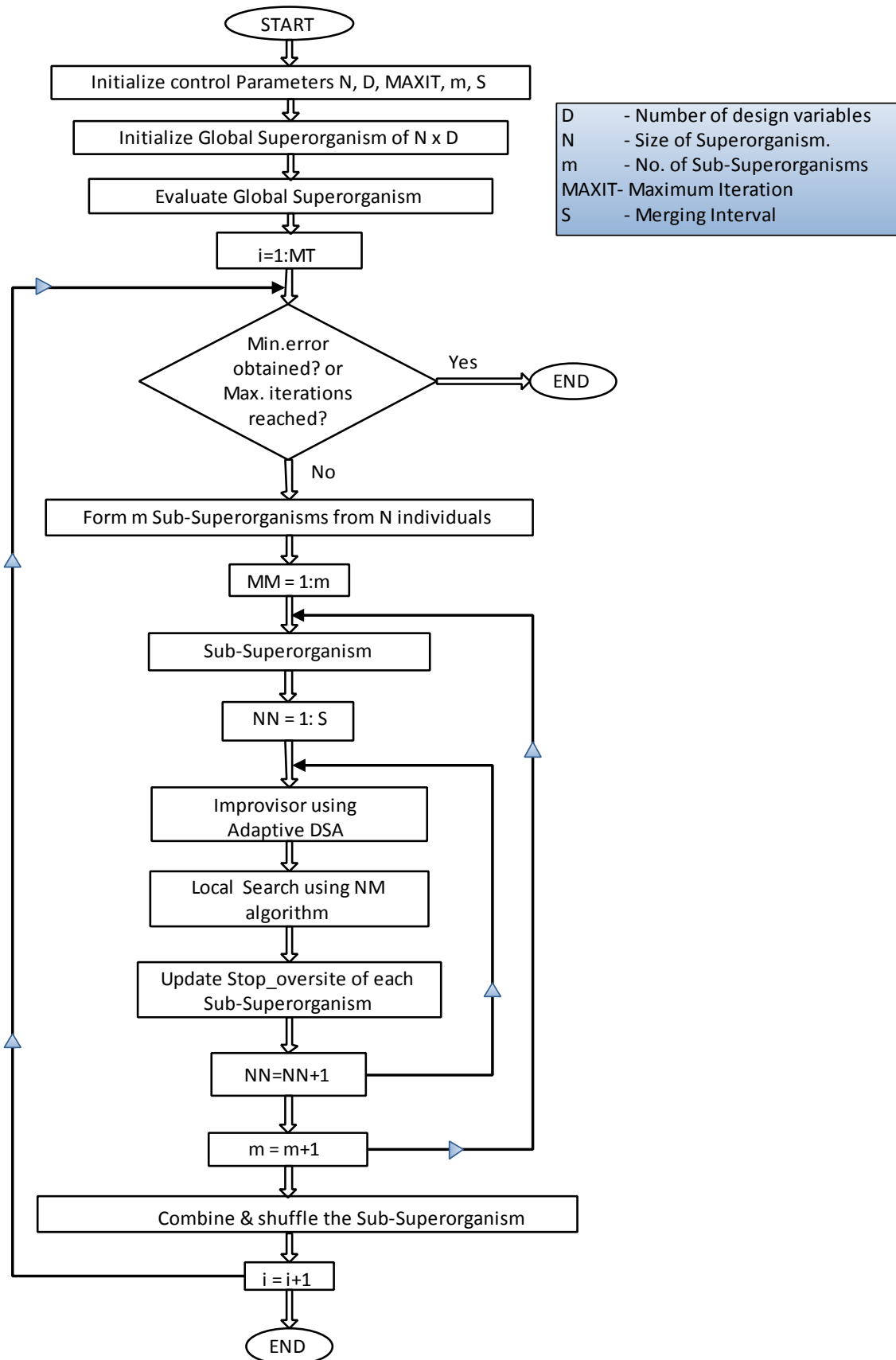


Fig. 4 Dynamic hybrid adaptive differential search (DHADS) algorithm

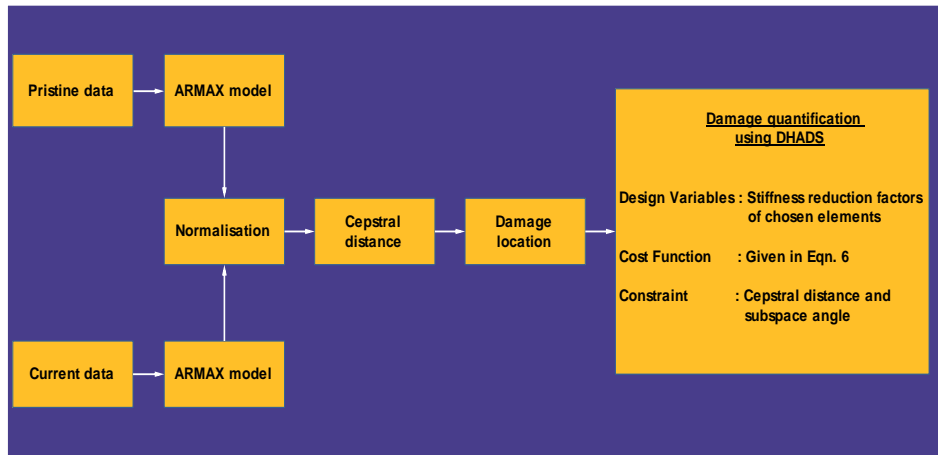


Fig. 5 Flowchart of the proposed damage diagnostic technique

dynamic characteristics like mass and stiffness of the structural system and therefore cannot consider the damping as well as loading present on the structural system. On the other hand, principal components are constructed from the structural dynamic time history responses and so they effectively represent all the dynamic characteristics of the system i.e., mass, stiffness, damping, dynamic load on the structure and the spatial location of the structure at which the dynamic load is acting, etc. Hence the PCA based sensor placement algorithm (PEfi) chooses the dynamically sensitive spatial locations on the structure for placement of the sensors. It is ensured that all the dynamic information present in the system is captured, as the important dynamic information lies in the principal directions, chosen based on the energy criteria. Accordingly, the Fisher information matrix with principal components can be defined as

$$\mathbf{Q}_c = \mathbf{U}_c^T \mathbf{W} \mathbf{U}_c \quad (14)$$

where \mathbf{U}_c is the dominant principal components partitioned to the candidate sensor set, and \mathbf{W} usually termed as weighting matrix and it is the inverse of the noise covariance matrix. In the present work, the weighting matrix, \mathbf{W} , is chosen as the identity matrix. An appropriate norm of the Fisher Information matrix is maximized in order to obtain the best state estimate. In the present work, the determinant of the Fisher information matrix is chosen as a norm for maximization. The same procedure of classical Efi is followed in the present optimal sensor placement technique using principal components (PEfi) to truncate the sensor positions. The contribution of each candidate sensor node is examined and the sensor position which has the least contribution to the determinant of the information matrix is chosen for truncation. This truncation is carried out in an iterative fashion similar to Efi until the desired targeted number of sensors is reached.

6. Numerical studies

Numerical experiments are conducted on examples of a simply supported beam, 15-storey framed structure and 12-

bay steel truss to validate the proposed technique. The results of the studies show the robustness of the algorithm to detect the time instance, the location and the extent of damage irrespective of the presence of noise and variability.

6.1 Simply supported beam

A simply supported beam is considered as the first numerical example with a span of 6 meters, discretized into 20 elements. The dimensions, the material and geometrical properties of the beam are shown in Figure 6.

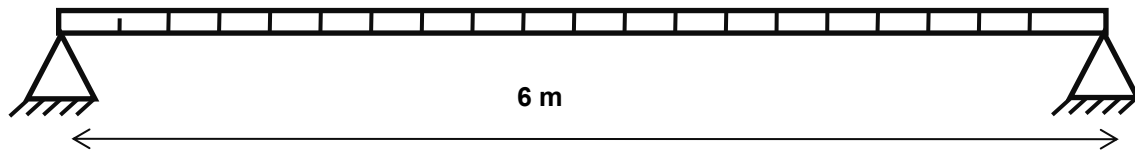
The external loading simulated is the random load in the form of Gaussian white noise. Under the conditions of simulated random loads and varying environmental conditions, Newmark's time integration scheme is used to compute the acceleration time-history response for every node with a sampling speed of 2000Hz. This simulates the data collected on a bridge girder on several time instants with varied operational (i.e., traffic levels & wind) loads. In addition to that, baseline datasets are generated with a range of temperatures from -15 to 50 degree centigrade.

The robustness of the structural damage diagnostic techniques to the effect of measurement noise is one of the important issues in real situations of SHM. Therefore, to investigate the effect of measurement noise on the robustness of the proposed approach, the computed time history measurements are contaminated with white Gaussian noise with zero mean statistics. A Gaussian random component is added to the noise-free acceleration time-history response to obtain the noisy sequences as follows:

$$\ddot{\mathbf{x}}_m = \ddot{\mathbf{x}} + \xi_p N_{noise} \sigma(\ddot{\mathbf{x}}) \quad (15)$$

Where ξ_p is the level of noise in percentage, N_{noise} is the standard normal distribution, $\sigma(\ddot{\mathbf{x}})$ is the standard deviation of the measured (computed) time-history response, uncorrupted with noise. In the present numerical studies, the random noise levels are varied by 5%, 8%, and 10%.

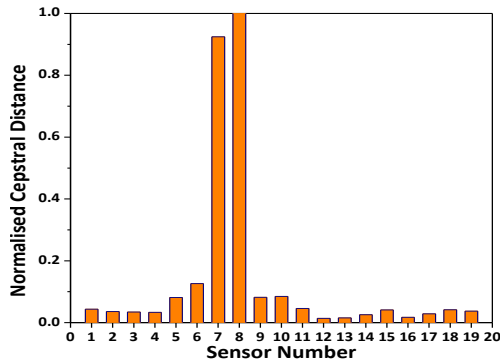
The generated baseline data is divided into 80 subsets of



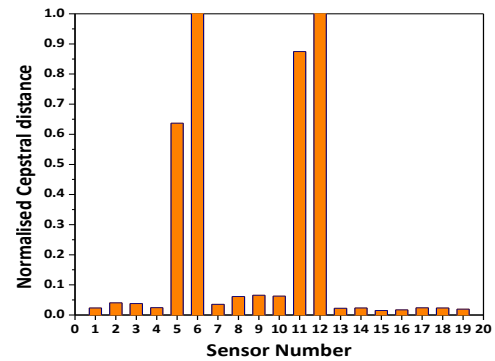
Elastic Modulus = 205 GPa; Cross sectional Area = 0.225m²

Mass Density = 7850 Kg/m³; Moment of Inertia = 0.000562 m⁴

Fig. 6 Simply supported beam



(a) Single damage of 12% at element 8



(b) Multiple damages of 10% and 15% at element 6 and 12 respectively

Fig. 7 Normalized cepstral distances of ARMAX models, indicating the location of damage in the SS beam with noise as 10%

1000 samples each and are contaminated with varying intensities of noise to perfectly simulate the measurement noise. The current data is generated in such a way that the structure is considered to be healthy for the specified initial period of time and beyond that, it encountered the damage. Element stiffnesses of a few elements of the FE model are reduced to simulate hypothetical damage scenarios for diagnosis. Single damage is simulated into simply supported beam girder after obtaining 20,000 samples of current data (i.e. after 10 sec), by reducing the stiffness of element 8 by 12% and multiple damages are simulated in elements 6 and 12 by 10% and 15% respectively.

Now, the damage diagnosis is carried out through the steps described in section 5.0 using the cepstral distance of two ARMAX models as a damage index. The normalized cepstral distance based damage index calculated for the single and multiple damages are shown in Figure 7. From the above-said figure, it is clear that the cepstral distance of ARMAX models is a good indicator of the spatial location of the damage. The damage index is not only capable of handling the operational variability and measurement noise efficiently, but also indicating the spatial location of damage robustly.

Once the spatial location is identified, the DHADS algorithm is employed to identify the quantity of damage. The design variables are the stiffness reduction factors corresponding to the elements which are identified by ARMAX models as shown in Figure 7. However, to demonstrate the effectiveness of the proposed DHADS algorithm, all the elements are considered as design

variables ignoring the identification of spatial locations by ARMAX models. Accordingly, the number of design variables (i.e. stiffness reduction factors of the elements) are considered as 20. The upper and lower limits of design variables are considered as 0.1 to 2.0 respectively in order to widen the search space. The cost function shown in Eqn. (6) is used in the formulated optimization problem using the variants of differential search algorithm described in section 4.

The following strategies during the optimization process in order to improve the convergence characteristics as well as the robustness of the proposed variants of the meta-heuristic algorithm are employed.

The optimization algorithm is started initially, as an unconstrained optimization problem and after few iterations, when the design variables converge, the cepstral distance and subspace angle of two datasets (i.e., the measured responses and numerically simulated responses) are employed as constraints. The imposition of the constraints after the initial few iterations will reduce the computational cost overheads and also helps the otherwise multimodal optimization problem converging towards the true solution under uncertainties associated with measurement noise and also modeling errors.

As mentioned earlier, a wider search space is used, by setting the upper and lower limits of the design variables (i.e., element stiffness coefficients) as 0.1 and 2.0. However, these upper limits and lower limits of the design variables are changed dynamically making use of the feedback from the previous iterations, during the execution

of the optimization algorithm. This dynamic reduction of search space during the execution of optimization algorithm is not new in the context for meta-heuristic algorithms and it is reported to be very effective in improving the accuracy of the converged solution, robustness and also substantially improves the computational performance (Rao *et al.* 2004). Hence it is proposed to adopt the similar concept of dynamic resetting of the search space. Initially, the proposed variants of the DS algorithms are executed with the present wider search space for the design variables. After the initially chosen random design variables are settled down, i.e. after few iterations say after every 15 iterations, the search space is reset based on the feedback from the solutions obtained from the previous fifteen iterations. The upper and lower limits are chosen by considering the weighted mean of the converged design variables during the past fifteen iterations and also the weighted variance. The new upper and lower limits are now set by considering the upper limit of each design variable as 'weighted mean value of the design variable + Five times the weighted variance of the design variable'. Similarly, the lower limit of the design variable is set as 'weighted mean value of the design variable - five times the weighted variance of the design variable'. The weighting function to arrive at the weighted mean and variance is taken as the ratio of fitness of each converged solution to the best fitness. This resetting of the upper and lower limits of the search space is carried out dynamically all through the optimization process for proposed variants of the DS algorithm.

The stiffness reduction factors identified with 10% of measurement noise using the three variants of differential search algorithm i.e. the conventional, two hybrid adaptive versions, and finally two algorithms with multi superorganisms with dynamic interaction i.e. DHADS algorithm is compared with the actual system parameters and the results are presented in Table 1. It can be observed from the results furnished in Table 1 that the stiffness reduction factors obtained using the proposed DHADS meta-heuristic algorithms are comparing very well with the true values. It can also be noted from the studies presented in Table 1 that the Nelder-Mead algorithm performs consistently well as a local search algorithm in hybrid DS and DHADS implementations when compared to Hook-Jeeves algorithm. The convergence characteristics of the three different implementations of differential search algorithm (i.e., CDS, HADS-NM and DHADS-NM) are evaluated and the best solution obtained in each evolution is shown in Figure 8. A careful look at Figure 8 indicates clearly that the proposed DHADS algorithm provides an optimal solution with faster convergence rate. Further, the DHADS algorithm converges in the least number of evolutions thus making it the fastest among all the algorithms compared in this paper.

The DHADS algorithm is a stochastic optimization algorithm and so there is no assurance that the final solutions arrived in every execution is the same. In view of this, the concept of practical reliability (PR) is used to assure the consistency of the proposed meta-heuristic algorithms. Practical reliability is defined as the percentage

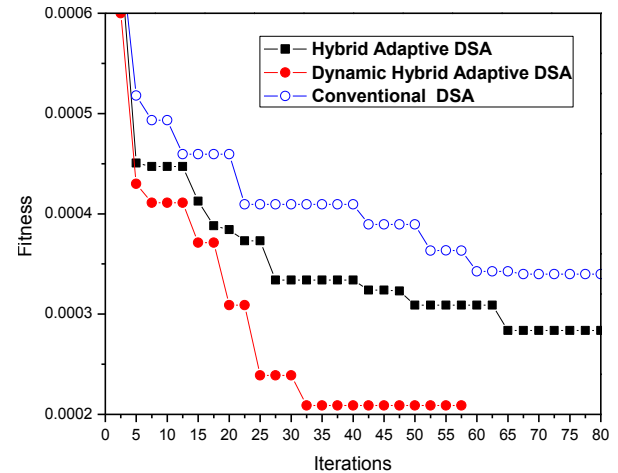


Fig. 8 Convergence plots of DHADS HADS and CDS algorithms

of converged solutions obtained using the DHADS stochastic algorithm with the exact stiffness and damping coefficients. However, a variation of 0.01 in the values of the exact solutions obtained is ignored. The evaluation of the practical reliability is performed by executing the stochastic algorithm for 30 different instances and by calculating the ratio of the maximum number of converged solutions that satisfy the above requirement to the number of independent executions of the algorithm. The practical reliability obtained for this example for the conventional differential search, hybrid differential search, HADS and proposed DHADS are found to be 0.89, 0.95, 0.99 respectively.

In order to measure the efficiency of the proposed algorithm, another measure which is the normalised price (NP) of each run (Jayalakshmi *et al.* 2018), is used in the present numerical experiments. The definition of price is formulated as the total number of function evaluations per complete execution of the proposed algorithm. The ratio of the mean price of the 30 executions of the proposed meta-heuristic algorithms to the practical reliability is defined as the normalised price. The normalised price of the conventional differential search, hybrid differential search, and DHADS algorithm are found to be 6375, 5850 and 3375 respectively. It can be concluded from the studies presented in Table 1 that the consistency coupled with faster convergence makes the proposed DHADS algorithm highly suitable for complex optimisation problems associated with structural system identification or damage quantification. It is also found to be highly immune to the measurement noise. The identification of the parameters is performed with an assumption that the mass matrix is exact. Nevertheless, in many instances, the precise values of the mass of each element are difficult to obtain. In view of this practical reason, it is assumed that the element mass is not known precisely and only known in the form of a normal distribution. Two case studies, where the mass matrix is assumed as known apriori and also the element mass as a normally distributed variable is considered for the investigation. The uncertainty in the values of the element

Table 1 Damage distribution of simply supported beam with damage in element 8 (12%) computed using variants of differential search (DS) algorithm with 10% measurement noise-multi constraint optimization

Element number	1	2	3	4	5	6	7	8	9	10
True stiffness parameters	1.000	1.000	1.000	1.000	1.000	1.000	1.000	0.880	1.000	1.000
Identified values Using conventional DSA(CDSA)	0.969	1.093	0.969	1.083	1.054	0.988	1.045	0.918	1.067	0.992
Identified values Using HADS-NM	0.977	0.982	0.977	1.094	0.966	1.018	1.098	0.872	1.044	1.056
Identified values using HADS -HJ	0.969	1.018	0.979	1.102	1.071	1.091	0.991	0.912	0.912	0.919
Identified values using DHADS -NM	0.996	1.009	1.008	0.996	1.008	0.996	0.994	0.879	1.007	0.997
Identified values using DHADS-HJ	1.021	1.074	0.982	0.904	1.034	1.021	0.992	0.904	1.044	0.992
Element number	11	12	13	14	15	16	17	18	19	20
True stiffness parameters	1.000	1.000	1.000	1.000	1.000	1.000	1.000	1.000	1.000	1.000
Identified values Using conventional DS(CDS)	0.964	0.988	1.043	1.067	0.967	0.984	0.982	0.991	0.932	0.962
Identified values Using HADS-NM	0.992	1.012	0.969	1.019	0.978	0.976	1.013	1.044	0.982	1.021
Identified values using HADS -HJ	0.943	0.985	0.978	1.102	1.049	1.009	0.989	0.947	1.014	0.992
Identified values using DHADS -NM	0.997	1.006	0.993	1.008	0.997	1.011	1.004	0.995	1.010	1.007
Identified values using DHADS-HJ	1.043	0.984	0.982	0.996	0.982	1.043	1.024	0.969	1.113	1.061

NM- Nelder Mead algorithm; HJ- Hooke & Jeeves algorithm

mass is simulated by considering them as normally distributed which are centered on the correct value with a 7% standard deviation of the corrected value.

To demonstrate the efficiency of the proposed algorithm to identify the stiffness parameter when the mass values follow the normal distribution, 12% damage is introduced in the 8th element and the acceleration data is generated. Using this generated data, the stiffness parameters are obtained for all the elements. The maximum, average errors in the identification of stiffness reduction factors of all elements in the beam are shown in Table 2. From the Table 2, it can be observed that the errors in the identification stiffness reduction factors with imprecise values of element masses (i.e. assumed to be known as the normal distribution) are marginally higher than those of the precisely known masses. These errors are due to the imprecise knowledge of the element mass. Nevertheless, such small error magnitudes indicate that the uncertainties associated with the mass of the structure have less influence on the identification of the stiffness reduction factors.

In order to test and verify the effectiveness of the proposed multi-constrained optimization model for identification of system parameters, the investigations are carried out, using all the proposed variants of DS algorithms without considering the two constraints (i.e., treating it as unconstrained optimization problem). The error in identification using precise values of elemental mass and with imprecise values of elemental mass is shown in Table 3. It can be observed from the results given in Table 3 that errors in the estimation of system parameters are consistently higher with the unconstrained optimization problem. Further, the errors in the estimation of system

parameters with imprecise values of elemental mass (i.e. mass assumed in the form of normal distribution) are found to be much higher. Apart from this, the number of function evaluations are consistently increased while using unconstrained optimization by about 24%. Hence it can be concluded from this investigation that using the two constraints in the proposed formulation increases the computational efficiency as well as the accuracy in the estimation of the system parameters.

In order to investigate the effectiveness of the proposed damage diagnostic technique, with limited instrumentation, 15, 10 and 7 numbers of sensors, optimally located using proposed PEfi algorithm discussed in the earlier section, are used. The damage index plots using ARMAX model are shown in Figure 9, considering 15, 10 and 7 sensors separately. It can be observed that the ARMAX model is able to locate the spatial location of multiple damages accurately.

Similarly, the damage localization is also carried out with limited instrumentation considering 15, 10 and 7 sensors with exactly known element mass and imprecisely known element mass, for varying noise levels in Table 4. It can be observed that the identification results are reasonably accurate, even with higher levels of noise. The average error works out to be, 1.11%, 2.44% and 2.80% when it is assumed that the element masses are precisely known for 15,10 and 7 sensors respectively with 10 percent noise. Similarly, the average errors are found to be 1.86%, 1.23% and 3.41%, with 15,10 and 7 sensors respectively, when mass assumed to be known as a normal distribution. The studies are carried out only using DHADS-NM algorithm using multi-constraint formulations.

Table 2 Error in the identification of stiffness parameters of the simply supported beam and with varied noise values using the variants of differential search implementations-multi constraint optimization

Name of the Algorithm	Noise-free		5% Noise		8% Noise		10% Noise	
	Max. Error	Avg. Error						
With element masses are known precisely								
CDSA	0.0144	0.0031	0.0196	0.0063	0.0207	0.0064	0.0213	0.0074
HADS-NM	0.0092	0.0024	0.0144	0.0052	0.0159	0.0057	0.0175	0.0063
HADS-HJ	0.0123	0.0026	0.0162	0.0067	0.0166	0.0061	0.0173	0.0082
DHADS-NM	0.0031	0.0004	0.0127	0.0044	0.0147	0.0049	0.0157	0.0057
DHADS-HJ	0.0041	0.0006	0.0142	0.0061	0.0165	0.0069	0.0147	0.0072
With element masses are known in the form of a normal distribution								
CDS	0.0253	0.0142	0.0266	0.0158	0.0215	0.0067	0.0222	0.0078
HADS-NM	0.0147	0.0065	0.0157	0.0068	0.0165	0.0059	0.0182	0.0066
HADS-HJ	0.0211	0.0083	0.0229	0.0086	0.0176	0.0069	0.0179	0.0086
DHADS-NM	0.0095	0.0044	0.0097	0.0046	0.0158	0.0051	0.0164	0.0062
DHADS-HJ	0.0091	0.0067	0.0109	0.0070	0.0161	0.0074	0.0174	0.0075

Table 3 Error in the identification of stiffness parameters of the simply supported beam and with varied noise values using different differential search implementations as an unconstrained optimization problem

Name of the Algorithm	Noise-free		5% Noise		8% Noise		10% Noise	
	Max. Error	Avg. Error						
With element masses are known precisely								
CDS	0.0267	0.0065	0.0244	0.0076	0.0238	0.0078	0.02622	0.0115
HADS-NM	0.0226	0.0053	0.0279	0.0073	0.0185	0.0072	0.02124	0.0083
HADS-HJ	0.0245	0.0053	0.0227	0.0075	0.0237	0.0072	0.02117	0.0091
DHADS-NM	0.0147	0.0025	0.0155	0.0049	0.0195	0.0065	0.01819	0.0074
DHADS-HJ	0.0153	0.0027	0.0218	0.0084	0.0188	0.0097	0.01832	0.0088
With element masses are known in the form of a normal distribution								
CDS	0.0319	0.0194	0.0331	0.0194	0.0284	0.0088	0.0277	0.0102
HADS-NM	0.0288	0.0088	0.0206	0.0077	0.0213	0.0072	0.0228	0.0081
HADS-HJ	0.0272	0.0113	0.0282	0.0107	0.0217	0.0085	0.0228	0.0111
DHADS-NM	0.0158	0.0057	0.0167	0.0069	0.0204	0.0067	0.0249	0.0184
DHADS-HJ	0.0171	0.0081	0.0145	0.0087	0.0253	0.0095	0.0227	0.0191

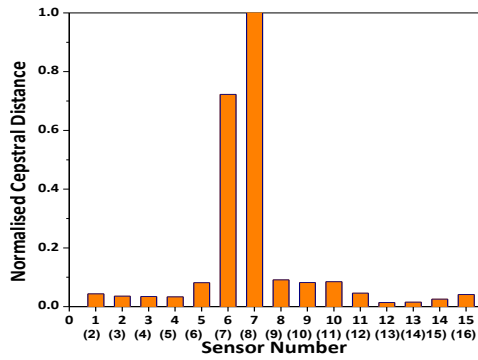
6.2 Fifteen storey framed structure

The 15-DOF framed structure which is idealized as a shear building model and shown in Figure 10, is the second numerical example. The frame is subjected to a lateral random excitation on the top-most storey. The mass of each floor is assumed as 1500 kg and the stiffness of each floor is considered as 5000 kN/m. The acceleration data generated by Newmark's time integration algorithm is corrupted by the addition of varying percentages (5%, 8%, and 10%) of Gaussian white noise as shown in Eqn. (15). The first six natural frequencies are 2.69Hz, 7.52 Hz, 12.26 Hz, 17.40Hz, 21.87 Hz and 26.06Hz respectively. Single damage is hypothetically simulated in the 3rd storey by reducing its stiffness by 15% assuming that the damage is set-in after 6 seconds with a sampling rate of 2000. The

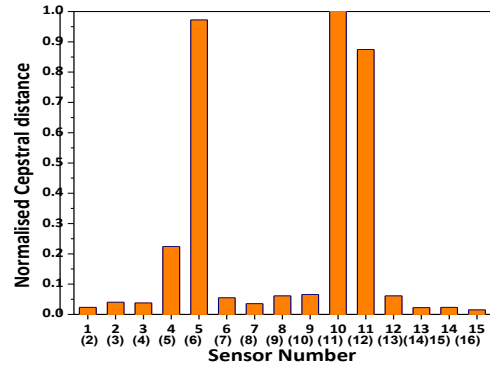
damage diagnosis is carried out through the steps described in section 5.0 using the damage index of the cepstral distance of ARMAX models. The cepstral distance of ARMAX models are evaluated and are shown in Figure 11(a). Similarly, multiple damages at 5th and 12th storey are simulated by reducing the stiffness by 16 percent of those original stiffness values.

The cepstral distance of ARMAX models related to the multiple damage case is evaluated for every sensor data and the magnitudes are shown in Figure 11(b) for the two levels of damage. Figure 11 clearly shows the location of single damage and also the multiple damages and therefore it is clear the cepstral distance index is a good indicator of the spatial location of the damage.

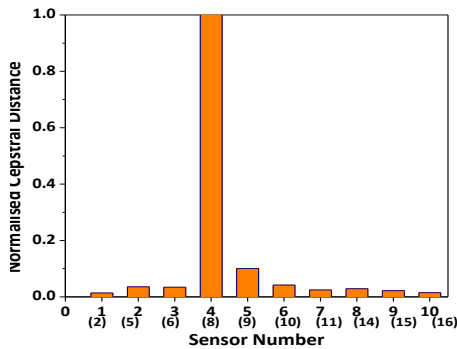
The damage distribution of the single and multiple damage cases are evaluated using the DHADS algorithm



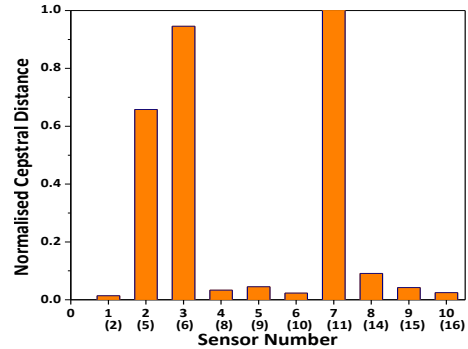
(a) Single Damage scenario with 15 optimal sensors



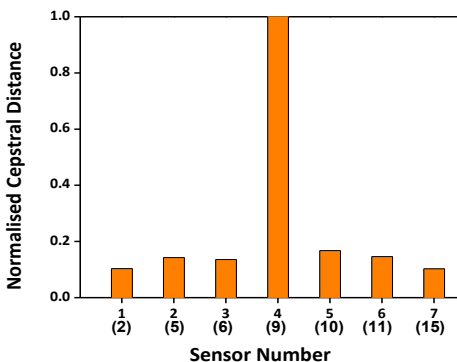
(b) Multiple Damage scenario with 15 optimal sensors



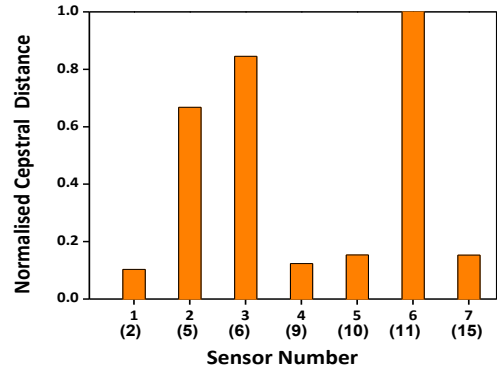
(c) Single Damage scenario with 10 optimal sensors



(d) Multiple Damage scenario with 10 optimal sensors



(e) Single Damage scenario with 7 optimal sensors



(f) Multiple Damage scenario with 7 optimal sensors

Fig. 9 Results of the numerical studies using simply supported beam with limited sensors

NOTE: The optimal sensor locations are shown in the X-axis of Figure 9(a)-9(f) and the corresponding original locations with a full set of sensors are shown within the parenthesis.

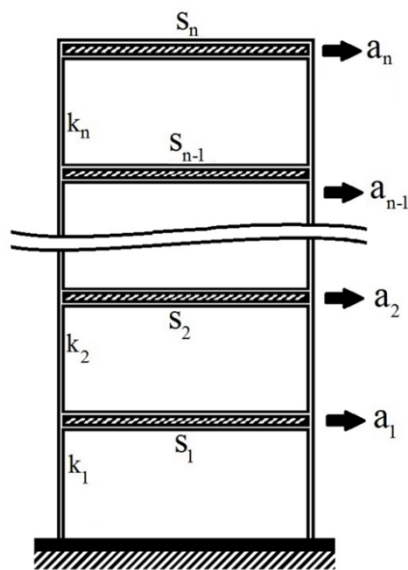
and the percentage of remaining stiffness identified by DHADS is shown in Table 5 for single and multiple damage case with 10% measurement noise. From Table 5, it can be clearly seen that the DHADS algorithm is efficient in identifying the parameters from the noisy signal. It can also be observed from the studies presented in Table 5 that the Nelder-mead algorithm performs consistently better as a local search algorithm when compared to Hooke and Jeeves algorithm. Similar to the first numerical example, the robustness of the technique to the modeling errors and the measurement noise is investigated and the values are shown in Table.6. From the table, it can be seen that the DHADS-

NM algorithm records the minimum average errors for varying noise levels irrespective of the knowledge of the element masses values.

In order to investigate the effectiveness of the proposed damage diagnostic technique, with limited instrumentation, the acceleration time-history measurements from 6 optimally located sensors, are used. The damage index plots using ARMAX model are shown in Figure 12, considering 6 optimally placed sensors for single damage at 3rd storey and multiple damages at 5th and 12 th storeys. From figure 12, it can be seen that the cepstral distance of ARMAX model is a good indicator of the location of damage even with the reduced sensor set.

Table 4 Error in the identification of stiffness parameters of the simply supported beam with limited instrumentation and with varied noise values using DHADS-NM with multi-constraint optimization formulations

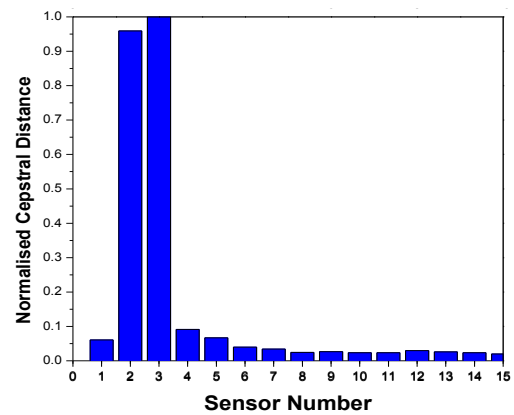
Number of Sensors	Sensor locations	Noise levels	With element masses are known precisely		With element masses are known in the form of a normal distribution	
			Max. Error	Avg. Error	Max Error	Avg. Error
15	[2, 3, 4, 5, 6, 7, 8, 9, 10, 11, 12, 13, 14, 15, 16]	0%	0.00134	0.00132	0.00952	0.06930
		5%	0.01213	0.00975	0.01298	0.01085
		8%	0.01341	0.00997	0.01482	0.01136
		10%	0.01429	0.01114	0.02146	0.01854
10	[2, 5, 6, 8, 9, 10, 11, 14, 15, 16]	0%	0.01229	0.00103	0.01639	0.01082
		5%	0.01888	0.00241	0.02149	0.01988
		8%	0.02121	0.01643	0.02917	0.02349
		10%	0.03123	0.02448	0.03458	0.01225
7	[2, 5, 6, 9, 10, 11, 15]	0%	0.01643	0.01034	0.02104	0.01037
		5%	0.02178	0.01315	0.02914	0.02149
		8%	0.03049	0.01979	0.03656	0.02286
		10%	0.04130	0.02801	0.04880	0.03414



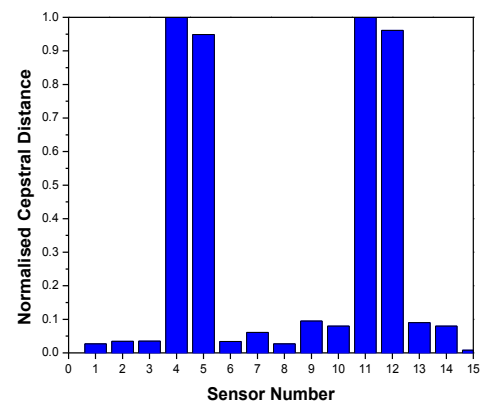
(a: acceleration time history; K: storey stiffness; S: storey)

Fig. 10 Framed structure with 15-storey

Similarly, the damage localization is also carried out with limited instrumentation for cases of exactly known element mass and imprecisely known element mass, for varying noise levels. The studies are carried out only using DHADS-NM algorithm using multi-constraint formulations. The error in the identification of stiffness parameters is shown in Table 7. It can be observed that the average error varies from 0.89% and 2.86% when it is assumed that the element masses are precisely known. Similarly, the average error varies from 0.98% to 2.98% when the mass is assumed to be known as a normal distribution. It is clear from the studies that the proposed technique is able to locate and quantify the damage even with limited measurements.



(a) Damage(15%) at 3rd storey



(b) Damage(16%) at 5th and 12th storey

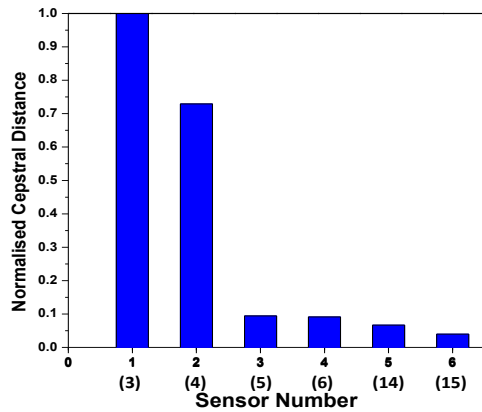
Fig. 11 Location of damage in the 15-storey shear building model using normalized cepstral distance

6.3 Twelve bay truss structure

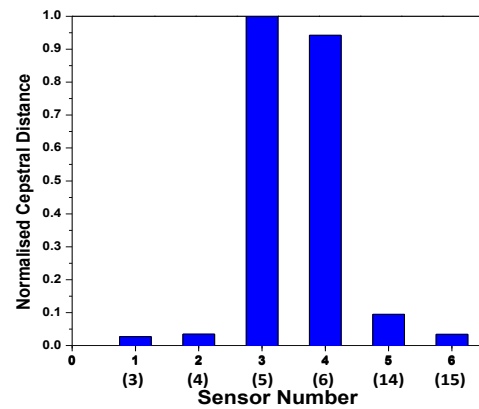
The third numerical study is a truss bridge with twelve bays and simply supported ends as shown in Figure 13. The

Table 5 True and identified parameters for 15- storey shear building, with single (15% damage at the 3rd storey) and multiple (16% damage at 5th and 12th storey) damage scenarios with 10% measurement noise

Storey number	1	2	3	4	5	6	7	8
True stiffness parameters	1.000	1.000	1.000	1.000	0.840	1.000	1.000	1.000
Identified values using CDSA	1.049	0.967	1.023	1.042	0.912	0.944	0.958	1.021
Identified values using HADS-NM	0.988	1.011	1.014	0.989	0.928	1.016	0.987	0.989
Identified values using HADS -HJ	1.013	1.041	0.968	0.944	1.011	1.022	0.962	0.966
Identified values using DHADS -NM	1.008	1.004	0.852	1.008	0.841	1.008	1.010	0.998
Identified values using DHADS-HJ	1.018	1.013	1.016	0.982	0.937	1.012	1.028	0.998
Storey number	9	10	11	12	13	14	15	
True stiffness parameters	1.000	1.000	1.000	0.840	1.000	1.000	1.000	
Identified values Using CDSA	0.969	0.988	1.017	0.929	0.944	1.021	1.020	
Identified values Using HADS-NM	1.009	1.012	0.989	0.924	1.017	0.984	1.011	
Identified values using HADS -HJ	1.036	0.967	1.027	0.921	1.032	0.947	0.988	
Identified values using DHADS -NM	1.008	1.011	1.004	0.841	1.007	0.993	0.996	
Identified values using DHADS-HJ	1.013	1.021	1.017	0.911	0.994	1.009	0.967	



(a) Damage(15%) at 3rd storey



(b) Damage(16%) at 5th and 12th storey

Fig. 12 Location of damage with limited sensors in the 15-storey shear building model using normalized cepstral distance
NOTE: The optimal sensor locations are shown in the X-axis of Figure 11(a)-11(b) and the corresponding original locations with a full set of sensors are shown within the parenthesis.

members of the truss, both the horizontal and the vertical, are of 0.0016m² as cross-sectional area and of 1m long. The truss is simulated to be supported by a pin joint and roller arrangement. The elastic modulus of the material and the mass density are, 200 GPa and 7.85×10³ kg /m³ respectively. The Rayleigh damping coefficients are 0.1523 and 4.6503 × 10⁻⁵ respectively. The external load is applied at nodes 11, 13 and 15 in the form of random excitation. The FE analysis of the model is used to extract the first few natural frequencies as 1.562, 5.172, 6.939, 11.986 and 17.727 Hz respectively.

The truss bridge is subjected to random loads. The acceleration data from the nodes(i.e. Node nos. 3,5,7,9,11,13,15,17,19,21,23), in the lower part of the truss, is computed from Newmark time-integration scheme, and white Gaussian noise is added in the form of a percentage of noise as shown in Eqn.(15). Two damage scenarios of 12% and 14% are simulated in the members of the 5th bay by reducing their stiffness values correspondingly.

The proposed damage diagnostic technique is employed

to identify the location of damage using the cepstral distance of the ARMAX models and are shown in Figure 14. From Figure 14, it can be clearly seen that the damage is located in the 5th bay and the members of that bay possess reduced stiffness values. Once the location of the damaged bay is identified, the damage distribution is identified using the DHADS algorithm.

The percentage of remaining stiffness obtained using the multi-population DHADS for 5% measurement noise is shown in Table 8. The values shown in Table 8, clearly, indicate the efficiency and the robustness of the proposed DHADS algorithm to identify the stiffness values in the truss bays in the presence of the measurement noise. It can also be observed from the results presented in Table 8 that the performance of the Nelder-Mead algorithm as local search algorithm in hybrid DS and DHADS algorithms is found to be superior when compared to Hooke and Jeeves algorithm.

The maximum and average errors of stiffness parameter identification of the conventional and the versions of DS

Table 6 Error in the identification of stiffness parameters of the 15 storey shear building with varying noise levels and modeling errors

Name of the Algorithm	Noise-free		5% Noise		8% Noise		10% Noise	
	Max. Error	Avg. Error						
With element masses are known precisely								
CDS	0.0129	0.003	0.019	0.0058	0.021	0.007	0.0196	0.0069
HADS-NM	0.0082	0.0021	0.0128	0.00463	0.0141	0.0051	0.0156	0.00561
HADS-HJ	0.0109	0.0029	0.0148	0.00595	0.0147	0.0054	0.0154	0.00728
DHADS-NM	0.0026	0.0003	0.0108	0.00375	0.0125	0.0042	0.01336	0.00485
DHADS-HJ	0.0034	0.0005	0.0119	0.00513	0.0138	0.0058	0.01234	0.00605
With element masses are known in the form of a normal distribution								
CDS	0.0228	0.0128	0.0240	0.01426	0.0194	0.0061	0.02003	0.00704
HADS-NM	0.0131	0.0058	0.0140	0.00606	0.0147	0.0054	0.0164	0.00584
HADS-HJ	0.0189	0.0074	0.0203	0.007641	0.0159	0.0061	0.01589	0.00763
DHADS-NM	0.0081	0.0038	0.0091	0.003916	0.0135	0.0043	0.01396	0.00528
DHADS-HJ	0.0076	0.0056	0.0099	0.00588	0.0135	0.0079	0.01462	0.0063

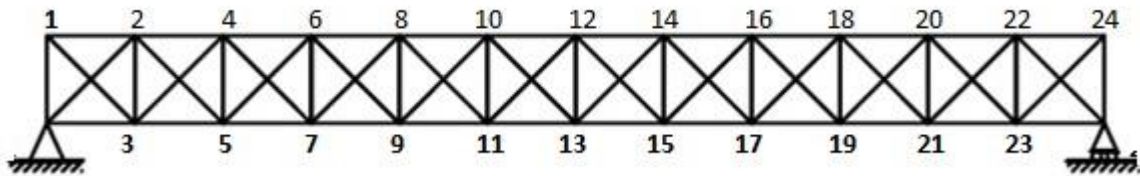


Fig. 13 12-bay steel truss bridge

Table 7 Error in the identification of stiffness parameters of 15 storey framed structure with limited instrumentation and with varied noise values using DHADS-NM with multi constraint optimization formulations

Number of Sensors	Sensor locations	Noise levels	With element masses are known precisely		With element masses are known in the form of a normal distribution	
			Max. Error	Avg. Error	Max Error	Avg. Error
6	[3, 4, 5, 6, 14, 15]	0%	0.0147	0.0089	0.0162	0.0098
		5%	0.0201	0.0101	0.0222	0.0113
		8%	0.0245	0.0198	0.0271	0.0211
		10%	0.0307	0.0286	0.0339	0.0298

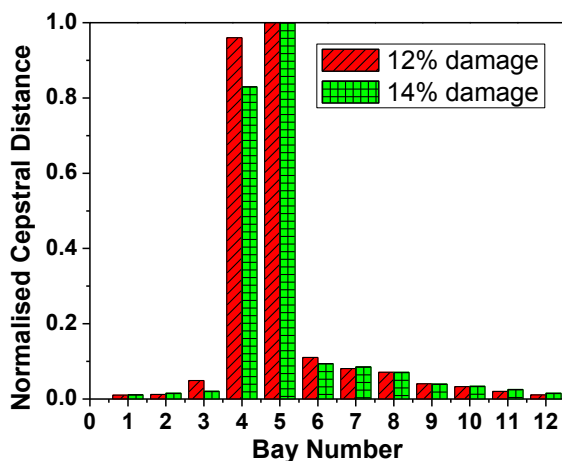


Fig. 14 Location of damage in 12-bay steel truss using normalised Cepstral distances of ARMAX models

under the effect of measurement noise and the variations in the mass of the elements are shown in Table 9 for this example. It can be seen clearly from Table 9, that the proposed DHADS-NM algorithm exhibits the lowest average error in identification of the stiffness parameters when compared the other techniques considered for the study.

In order to investigate the effectiveness of the proposed damage diagnostic technique, with limited instrumentation, 7 and 5 numbers of optimally located sensors are used. The damage index plots using ARMAX model are shown in Figure 15, considering 7 and 5 numbers of optimally placed sensors. The damage localization is also carried out with limited instrumentation considering 7 and 5 optimally placed sensors with exactly known element mass and imprecisely known element mass, for varying noise levels. The identification results are shown in Table 10, from

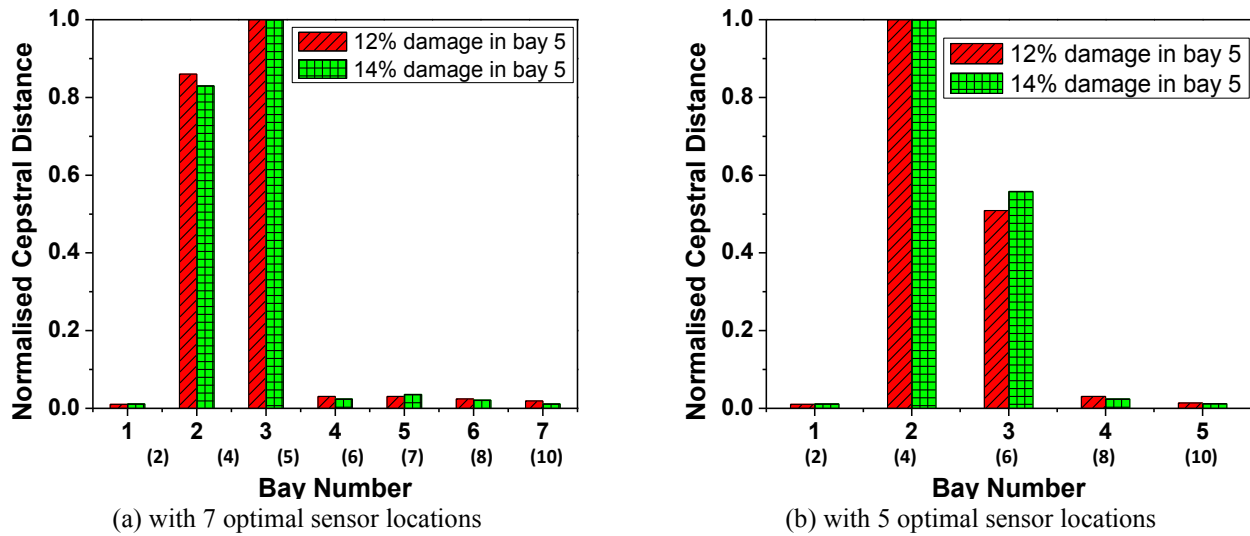


Fig. 15 Damage location in 12-bay steel truss using normalised Cepstral distances of ARMAX models

NOTE: The optimal sensor locations are shown in the X-axis of Figure 15(a)-15(b) and the corresponding original Bay numbers with a full set of sensors are shown within the brackets.

Table 8 Damage distribution of 12- bay truss computed with 12% damage at 5th bay using the variants of DSA algorithms with 5% measurement noise - multi constraint optimization

Bay number	1	2	3	4	5	6	7	8	9	10	11	12
True stiffness parameters	1.000	1.000	1.000	0.93	0.880	1.000	1.000	1.000	1.000	1.000	1.000	1.000
Identified values Using conventional CDSA	1.016	0.965	1.021	0.884	0.831	0.984	1.009	0.992	0.921	1.014	0.923	0.963
Identified values Using HADS-NM	1.011	0.986	0.984	0.918	0.924	1.023	0.998	1.014	0.957	0.954	1.023	0.989
Identified values using HADS-HJ	1.018	0.944	0.969	0.892	0.856	1.036	1.014	0.967	0.914	1.021	1.018	1.011
Identified values using DHADS-NM	0.997	1.011	0.994	0.941	0.879	1.008	0.995	1.009	0.992	1.007	1.009	0.998
Identified values using DHADS-HJ	0.967	0.936	1.021	0.912	0.981	1.032	0.935	1.019	0.961	1.008	1.004	0.989

NM- Nelder Mead algorithm; HJ- Hooke & Jeeves algorithm

which it can be observed that the maximum average error in identification of the parameters with 10% noise level is 2.79%. From the results, it can be clearly found, that the proposed ARMAX based technique to locate and DHADS-NM technique to quantify the damage, perform well even with the limited sensor arrangements on the structure.

5. Conclusions

In this paper, a damage diagnostic technique to quantify the extent of the damage for structural health monitoring of civil engineering structures using time series models is presented. Even though damage diagnostic techniques using time series models are presented earlier to identify the exact time instant and the precise location, quantifying the damage using the time series model is not reported widely. The time instant and the location of damage are identified using the damage index, which works basically on the distance between two ARMAX models using Cepstrum concept. The subsequent process of evaluating the intensity

of damage at the identified locations is considered as an inverse identification problem, which is a multi-modal complex problem to solve.

In view of this, in this paper, the inverse problem associated with damage quantification is formulated for the first time as a multi-constraint optimization technique in order to improve the robustness and also the convergence characteristics. The inverse problem on hand is usually a multimodal optimization problem if it is free from constraints due to varying levels of measurement noise and also modeling errors. In view of this, two constraints in the form of the cepstral distance between ARMAX models and also the subspace angle spanned by the measured responses of the structure after damage and the numerically simulated responses are imposed in the proposed optimization algorithm, in order to drive the otherwise multimodal optimization problem to converge to the true solution. The proposed variant of DS algorithm, built with hybrid and adaptive features, multiple small superorganisms is found to be faster and effective to solve the complex optimization problem associated with the identification of system

Table 9 Error in the identification of stiffness parameters of the 12-bay truss bridge with varying noise levels and modeling errors-multi constraint optimization

Name of the Algorithm	Noise-free		5% Noise		8% Noise		10% Noise	
	Max. Error	Avg. Error						
With element masses are known precisely								
CDS	0.0149	0.0035	0.0203	0.00645	0.0216	0.0067	0.02175	0.00754
HDS-NM	0.0087	0.0026	0.0133	0.004793	0.0152	0.0061	0.0161	0.00583
HDS-HJ	0.0102	0.0024	0.0141	0.005761	0.0137	0.0051	0.01436	0.00681
DHADS-NM	0.0024	0.0003	0.0102	0.00352	0.0118	0.0039	0.01256	0.00456
DHADS-HJ	0.0035	0.0007	0.0118	0.00500	0.0135	0.0059	0.01205	0.00592
With element masses are known in the form of a normal distribution								
CDS	0.0258	0.0146	0.0271	0.01611	0.0219	0.0068	0.02264	0.00795
HDS-NM	0.0135	0.0059	0.0147	0.006259	0.0153	0.0052	0.01679	0.00608
HDS-HJ	0.0176	0.0069	0.0191	0.007138	0.0149	0.0057	0.01489	0.00716
DHADS-NM	0.0076	0.0035	0.0089	0.00368	0.0126	0.0041	0.01312	0.00496
DHADS-HJ	0.0075	0.0055	0.0099	0.00574	0.0132	0.0077	0.01426	0.00615

Table 10 Error in the identification of stiffness parameters of a truss bridge with limited instrumentation and with varied noise values using DHADS-NM with multi constraint optimization formulations

Number of Sensors	Sensor locations	Noise levels	With element masses are known precisely		With element masses are known in the form of a normal distribution	
			Max. Error	Avg. Error	Max Error	Avg. Error
7	[5, 9,11,13,15,17,21] on Bay number [2,4,5,6,7,8,10]	0%	0.0167	0.0094	0.0187	0.0106
		5%	0.0231	0.0101	0.0259	0.0113
		8%	0.0287	0.0198	0.0321	0.0222
		10%	0.0342	0.0246	0.0383	0.0276
5	[5, 9,13,17,21] on Bay number [2,4,6,8,10]	0%	0.0169	0.0076	0.0189	0.0085
		5%	0.0233	0.0128	0.0261	0.0146
		8%	0.0271	0.0191	0.0316	0.0217
		10%	0.0391	0.0245	0.0439	0.0279

parameters. The proposed technique uses the measured acceleration time history corrupted with measurement noise and also the system with the known imprecise values of mass. The adaptive variation of search space suggested in the proposed algorithm helps in improving the converge characteristics.

A simply supported beam is used for numerical simulation studies by considering the varied loads, temperature variability and measurement noise. Studies presented in this paper clearly indicate that the exact time instant of damage and also multiple spatial locations of damage are robustly identified by the proposed algorithm, even with environmental variability, practical measurement noise levels and even with modeling errors. Apart from the above, the proposed algorithm is also validated using a 15-storey shear building model and a 12-bay steel truss with their recordings contaminated with varying levels of measurement noise and also with modeling errors.

The studies presented in this paper clearly suggest the following:

- The cepstral distance measure is an efficient indicator of the spatial location of damage, even with limited measurements.
- The multi-constraint optimization technique using DHADS, proposed in this paper to evaluate the intensity of damage, is found to be faster in convergence and its superior performance is evident from the measures such as practical reliability and normalized price.
- The hybrid algorithms integrating with an efficient local search algorithm improve the convergence characteristics
- The Nelder-Mead algorithm seems to be more effective when compared to Hooke and Jeeves algorithm as a local search algorithm.

References

- Akhras, G., Asanuma, H., Balageas, D., Bannister, M., Boller, C., Buderath, M. and Cawley, P. (2008), *Proceedings of the 4th*

- European Workshop on Structural Health Monitoring*, Cracow, Poland. July.
- Balsamo, L., Betti, R. and Beigi, H. (2014), "A structural health monitoring strategy using cepstral features", *J. Sound Vib.*, **333**(19), 4526-4542. <https://doi.org/10.1016/j.jsv.2014.04.062>.
- Bagheri, A., Ghodrati Amiri, G., Khorasani, M. and Bakhshi, H. (2011), "Structural damage identification of plates based on modal data using 2D discrete wavelet transform", *Struct. Eng. Mech.*, **40**(1), 13-28. <https://doi.org/10.12989/sem.2011.40.1.013>.
- Bao, C., Hao, H., Li, Z. X. and Zhu, X. (2009), "Time-varying system identification using a newly improved HHT algorithm", *Comput. Struct.*, **87**(23-24), 1611-1623. <https://doi.org/10.1016/j.compstruc.2009.08.016>.
- Björck, Å. and Golub, G.H. (1973), "Numerical methods for computing angles between linear subspaces", *Math. Comput.*, **27**(123), 579-594. <https://doi.org/10.1090/S0025-5718-1973-0348991-3>.
- Carden, E.P. and Brownjohn, J.M. (2008), "ARMA modelled time-series classification for structural health monitoring of civil infrastructure", *Mech. Syst. Signal Proc.*, **22**(2), 295-314. <https://doi.org/10.1016/j.ymssp.2007.07.003>.
- Chakraborty, D. and Dutta, A. (2005), "Optimization of FRP composites against impact induced failure using island model parallel genetic algorithm", *Compos. Sci. Technol.*, **65**(13), 2003-2013. <https://doi.org/10.1016/j.compscitech.2005.03.016>.
- Cheng, J.J., Guo, H.Y. and Wang, Y.S. (2017), "Structural Nonlinear Damage Detection Method Using AR/ARCH Model", *J. Struct. Stability Dynam.*, **17**(8), <https://doi.org/10.1142/S0219455417500833>.
- Civicioglu, P. (2012), "Transforming geocentric Cartesian coordinates to geodetic coordinates by using differential search algorithm", *Comput. Geosci.*, **46**, 229-247. <https://doi.org/10.1016/j.cageo.2011.12.011>.
- Doebling, S.W., Farrar, C.R. and Prime, M.B. (1998), "A summary review of vibration-based damage identification methods", *Shock Vib. Digest*, **30**(2), 91-105.
- Dosiek, L. and Pierre, J. W. (2013), "Estimating electromechanical modes and mode shapes using the multichannel ARMAX model", *IEEE Transactions Power Syst.*, **28**(2), 1950-1959. <https://doi.org/10.1109/TPWRS.2013.2252928>.
- Feeny, B. F. and Liang, Y. (2003), "Interpreting proper orthogonal modes of randomly excited vibration systems", *J. Sound Vib.*, **265**(5), 953-966. [https://doi.org/10.1016/S0022-460X\(02\)01265-8](https://doi.org/10.1016/S0022-460X(02)01265-8).
- Hamidian, D., Salajegheh, E. and Salajegheh, J. (2018), "Damage detection technique for irregular continuum structures using wavelet transform and fuzzy inference system optimized by particle swarm optimization", *Struct. Eng. Mech.*, **67**(5), 457-464. <https://doi.org/10.12989/sem.2018.67.5.457>.
- Homaei, F., Shojaee, S. and Ghodrati Amiri, G. (2014), "A direct damage detection method using multiple damage localization index based on mode shapes criterion", *Struct. Eng. Mech.*, **49**(2), 183-202. <http://dx.doi.org/10.12989/sem.2014.49.2.183>.
- Hooke, R. and Jeeves, T. A. (1961), "'Direct Search' Solution of Numerical and Statistical Problems", *JACM*, **8**(2), 212-229. <https://doi.org/10.1145/321062.321069>.
- Hore, S., Chatterjee, S., Sarkar, S., Dey, N., Ashour, A. S., Balas-Timar, D. and Balas, V. E. (2016), "Neural-based prediction of structural failure of multistoried RC buildings", *Struct. Eng. Mech.*, **58**(3), 459-473. <http://dx.doi.org/10.12989/sem.2016.58.3.459>.
- Huynh, D., He, J. and Tran, D. (2005), "Damage location vector: A non-destructive structural damage detection technique", *Comp. Struct.*, **83**(28-30), 2353-2367. <https://doi.org/10.1016/j.compstruc.2005.03.029>.
- Jayalakshmi, V., Lakshmi, K. and Rao, A.R.M. (2018), "Dynamic force reconstruction techniques from incomplete measurements", *J. Vib. Control*, **24**(22), 5321-5344. <https://doi.org/10.1177/1077546317752709>.
- Johnson, D.S. and McGeoch, L.A. (1997), "The travelling salesman problem: A case study in local optimization", *Local Search in Combinatorial Optimization*, Wiley, London, United Kingdom. 215-310.
- Kammer, D.C. (2005), "Sensor Set Expansion for Modal Vibration Testing", *Mech. Syst. Signal Process.*, **19**(4), 700-713. <https://doi.org/10.1016/j.ymssp.2004.06.003>.
- Koh, C. G. and Perry, M. J. (2009), *Structural Identification and Damage Detection using Genetic Algorithms: Structures and Infrastructures Book Series*, CRC Press, New Jersey, USA. 6.
- Laier, J.E. and Morales, J.D. (2009), "Improved genetic algorithm for structural damage detection", *Computational Structural Engineering, Proceedings of the International Symposium on Computational Structural Engineering*, Shanghai, China, June. 833-839. https://doi.org/10.1007/978-90-481-2822-8_91.
- Lakshmi, K. and Rama Mohan Rao, A. (2014), "A robust damage-detection technique with environmental variability combining time-series models with principal components", *Nondestructive Testing Evaluation*, **29**(4), 357-376. <https://doi.org/10.1080/10589759.2014.949709>.
- Lakshmi, K. and Rama Mohan Rao, A. (2015), "Damage identification technique based on time series models for LANL and ASCE benchmark structures", *Insight-Non-Destructive Testing and Condition Monitoring*, **57**(10), 580-588. <https://doi.org/10.1784/insi.2015.57.10.580>.
- Lakshmi, K. and Rao, A.R.M. (2016), "Structural damage detection using ARMAX time series models and cepstral distances", *Sādhanā*, **41**(9), 1081-1097. <https://doi.org/10.1007/s12046-016-0534-3>.
- Li, Y. Y. and Chen, Y. (2013), "A review on recent development of vibration-based structural robust damage detection", *Struct. Eng. Mech.*, **45**(2), 159-168. <https://doi.org/10.12989/sem.2013.45.2.159>.
- Liu, J., Wu, C., Wu, G. and Wang, X. (2015), "A novel differential search algorithm and applications for structure design", *Appl. Math. Comput.*, **268**, 246-269. <https://doi.org/10.1016/j.amc.2015.06.036>.
- Nobahari, M. and Seyedpoor, S.M. (2013), "An efficient method for structural damage localization based on the concepts of flexibility matrix and strain energy of a structure", *Struct. Eng. Mech.*, **46**(2), 231-244. <https://doi.org/10.12989/sem.2013.46.2.231>.
- Oppenheim, A. V. and Schaffer, R. W. (1975), "Digital filter design techniques", *Digital Signal Processing*, Prentice-Hall, New Jersey, USA. 585.
- Rao, A.R.M. and Ganesh, A. (2008), "Optimal sensor placement techniques for system identification and health monitoring of civil structures", *J. Smart Struct. Syst.*, **4**(4), 465-492. <https://doi.org/10.12989/sss.2008.4.4.465>.
- Rao, A.R.M. and Lakshmi, K. (2011), "Discrete hybrid PSO algorithm for design of laminate composites with multiple objectives", *J. Reinforced Plastics Compos.*, **30**(20), 1703-1727. <https://doi.org/10.1177/0731684411417198>.
- Rao, A.R.M., Rao, T.V.S.R.A. and Dattaguru, B. (2004), "Generating optimised partitions for parallel finite element computations employing float-encoded genetic algorithms", *Comput. Model. Eng. Sci.*, **5**(3), 213-234.
- Rao, A.R.M., Lakshmi, K. and Venkatachalam, D. (2012), "Damage diagnostic technique for structural health monitoring using POD and self-adaptive differential evolution algorithm", *Comp. Struct.*, **106**, 228-244. <https://doi.org/10.1016/j.compstruc.2012.05.009>.
- Rao, A.R.M. and Lakshmi, K. (2012), "Optimal design of stiffened laminate composite cylinder using a hybrid SFL algorithm", *J. Compos. Mater.*, **46**(24), 3031-3055. <https://doi.org/10.1177/0021998311435674>.

- Rao, A.R.M., Lakshmi, K. and S.K. Kumar. (2015), "Detection of delamination in laminated composites with limited measurements combining PCA and dynamic QPSO", *Adv. Eng. Software*, **86**, 85-106. <https://doi.org/10.1016/j.advengsoft.2015.04.005>.
- Seyedpoor, S.M. and Montazer, M.A. (2016), "A damage identification method for truss structures using a flexibility-based damage probability index and differential evolution algorithm", *Inverse Problems Sci. Eng.*, **24**(8), 1303-1322. <https://doi.org/10.1080/17415977.2015.1101761>.
- Sohn, H. and Farrar, C.R. (2001), "Damage diagnosis using time series analysis of vibration signals", *Smart Mater. Struct.*, **10**(3), 446. <https://doi.org/10.1088/0964-1726/10/3/304>.
- Sohn, H., Farrar, C.R., Hemez, F. M., Shunk, D.D., Stinemates, D. W., Nadler, B.R. and Czarnecki, J.J. (2003), "A review of structural health monitoring literature: 1996–2001", Los Alamos National Laboratory, USA.
- Tang, H., Suqi, L., Chunfeng, W and Songtao, X. (2018), "Experimental Verification of the Statistical Time-Series Methods for Diagnosing Wind Turbine Blades Damage", *J. Struct. Stability Dynam.*, **19**(1), <https://doi.org/10.1142/S021945541940008X>.
- Worden, K. and Farrar, C.R. (2007), "Theme issue: Structural health monitoring", *Philosophical Transactions Royal Soc. A*, **365**(1861), 299–632.
- Yu, L. and Zhu, J. H. (2015), "Nonlinear damage detection using higher statistical moments of structural responses", *Struct. Eng. Mech.*, **54**(2), 221-237. <https://doi.org/10.12989/sem.2015.54.2.221>.
- Zheng, H. and Mita, A. (2008), "Damage indicator defined as the distance between ARMA models for structural health monitoring", *Struct. Control Health Monitor.*, **15**(7), 992-1005. <https://doi.org/10.1002/stc.235>.

APPENDIX-A

A.1 Cepstral distance between ARMAX models

The power cepstrum is the logarithm of the power spectrum $P(z)$, subjected to inverse Fourier transform (Oppenheim and Schaffer 1975):

$$\begin{aligned} \log P(z) &= \log \{ \sigma^2 H(z) \bar{H}(z^{-1}) \} \\ &= \sum_{k \in \mathbb{Z}} cc(k) z^{-k} \end{aligned} \quad (\text{A1})$$

Where $cc(k)$ are the cepstrum coefficients, σ^2 is the variance of the white noise process possessing zero-mean and $H(z)$ is the transfer function of the system. An ARMAX process is represented as follows:

$$\begin{aligned} A(q^{-1})x[k] &= B(q^{-1})u[k - n_k] \\ &+ C(q^{-1})e_x[k] \end{aligned} \quad (\text{A2})$$

In Z domain, the transfer function of the system's ARMAX process can be represented in the following form (Dosiek and Pierre 2013):

$$H(Z) = [A^{-1}(Z)B(Z) \quad A^{-1}(Z)C(Z)] \quad (\text{A3})$$

Where

$$A^{-1}(q) = \frac{1}{|A(q)|} \text{adj}[A(q)];$$

$A(q) = I + A_1 q^{-1} + \dots + A_{n_a} q^{-n_a}$ is the AR polynomial matrix; $B(q) = B_0 + B_1 q^{-1} + \dots + B_{n_b} q^{-n_b}$ is the input polynomial matrix and $C(q) = I + C_1 q^{-1} + \dots + C_{n_c} q^{-n_c}$ is the MA polynomial matrix with orders n_a , n_b and n_c respectively.

A close look at the second part of the transfer function shows the AR and MA components of the system. If these components are in terms of poles $\alpha(i)$ and zeros $\beta(i)$, the transfer function resembles that of a stable, minimum ARMA process in the Z-domain as

$$H(z) = \frac{\sum_{i=0}^{n_c} c(i)z^{-i}}{\sum_{i=0}^{n_a} a(i)z^{-i}} = \frac{\prod_{i=1}^{n_c} (1 - \beta(i)z^{-i})}{\prod_{i=1}^{n_a} (1 - \alpha(i)z^{-i})} \quad (\text{A4})$$

Therefore, now, for any two ARMAX models AM_1 , and AM_2 , with the corresponding cepstrum coefficients $cc1(n)$ and $cc2(n)$, the cepstral distance becomes:

$$d(AM_1, AM_2)^2 = \sum_{n=1}^{\infty} n |\alpha_1(n) - \alpha_2(n)|^2 \quad (\text{A5})$$

where $cc(n)$ are the coefficients of the cepstrum given in

terms of poles and zeros

$$cc(n) = \begin{cases} \frac{1}{|n|} \left\{ \sum_{i=1}^{n_a} \alpha^{|n|}(i) - \sum_{i=1}^{n_c} \beta^{|n|}(i) \right\}, & n \neq 0 \\ \log \sigma^2, & n = 0 \end{cases} \quad (\text{A6})$$

A.2 Subspace angle

Angles between Subspaces

One way to compare hyperplane is to use the concept of angles between the two subspaces. This concept allows quantifying the spatial coherence between two time-history blocks of an oscillating system. Let $A \in \mathbb{R}^{n_s \times p}$ and $B \in \mathbb{R}^{n_s \times q}$ each with linearly independent columns. The principal angles between two subspaces are a generalization of an angle between two vectors, and their number is equal to the dimension of the smallest subspace. An algorithm for the computation of principal angles proposed by Bjorck and Golub (1973) using QR factorization and singular value decomposition can be used for this purpose. First, a QR factorization allows computing the orthonormal bases of A and B.

$$\begin{aligned} A &= Q_A R_A & Q_A &\in \mathbb{R}^{n_s \times p} \\ B &= Q_B R_B & Q_B &\in \mathbb{R}^{n_s \times q} \end{aligned} \quad (\text{A7})$$

Thus, the singular values of $Q_A^T Q_B$ define the q cosines of the principal angles θ_i between A and B.

$$\begin{aligned} SVD(Q_A^T Q_B) &\rightarrow \text{Diag}(\cos(\theta_i)) \\ &i=1, \dots, q \end{aligned} \quad (\text{A8})$$

The largest angle allows quantifying how the subspaces A and B are globally different. The responses of the subspaces between measured data (i.e. from the structure with identified location of damage) and the analytically simulated response, for evaluating the damage distribution are compared by computing the principal angles.